Biochimica et Biophysica Acta 1817 (2012) 26–43

Contents lists available at ScienceDirect

Biochimica et Biophysica Acta

journal homepage: www.elsevier.com/locate/bbabio

Review

Charge separation in Photosystem II: A comparative and evolutionary overview ☆

Tanai Cardona [a], Arezki Sedoud [a,b], Nicholas Cox [c], A. William Rutherford [a,b,*]

[a] Institut de Biologie et Technologies de Saclay, URA 2096 CNRS, CEA Saclay, 91191 Gif-sur-Yvette, France
[b] Molecular Biosciences, Imperial College, London SW7 2AZ, UK
[c] MPI für Bioanorganische Chemie, Stiftstrasse 34-36/D-45470 Mülheim an der Ruhr, Germany

ARTICLE INFO

Article history:
Received 29 March 2011
Received in revised form 22 July 2011
Accepted 23 July 2011
Available online 30 July 2011

Keywords:
Photosystem II
Charge separation
Quinone
Type II reaction center
Evolution
Photoprotection

ABSTRACT

Our current understanding of the PSII reaction centre owes a great deal to comparisons to the simpler and better understood, purple bacterial reaction centre. Here we provide an overview of the similarities with a focus on charge separation and the electron acceptors. We go on to discuss some of the main differences between the two kinds of reaction centres that have been highlighted by the improving knowledge of PSII. We attempt to relate these differences to functional requirements of water splitting. Some are directly associated with that function, e.g. high oxidation potentials, while others are associated with regulation and protection against photodamage. The protective and regulatory functions are associated with the harsh chemistry performed during its normal function but also with requirements of the enzyme while it is undergoing assembly and repair. Key aspects of PSII reaction centre evolution are also addressed. This article is part of a Special Issue entitled: Photosystem II.

1. Introduction

1.1. A general introduction: charge separation in photosynthetic reaction centres

When chlorophyll absorbs light, an electron is promoted from the highest occupied molecular orbital to the lowest or second lowest unoccupied molecular orbital. The energy in red light corresponds to the transition up to the first excited singlet state. The greater energy in blue light is sufficient for the electron to reach the higher excited singlet state but this state decays rapidly, with the loss of some energy, to form the longer-lived, first excited state. Thus the energy available for photochemistry corresponds to that of the red photon (e.g. 680 nm = 1.82 eV). The energy of green light does not correspond to that needed to promote a valence electron to an excited state and thus it is not absorbed but instead reflected or transmitted. Hence, chlorophyll is green.

Nearly all of the chlorophyll in photosynthetic organisms is bound to proteins of two types: antenna proteins and reaction centre proteins. Most chlorophylls are in antenna proteins where they play light-collecting roles. When excited by a photon of light, an antenna chlorophyll will rapidly pass on the excitation to one of the adjacent chlorophylls to which it is electronically coupled. The excitation can visit a large number of chlorophylls during the lifetime of the excited state (the fluorescence lifetime for chlorophyll is 5 ns [1]). The coupled chlorophylls can be within the same protein or in adjacent proteins that are in close physical contact. However, when the excitation arrives on a particular chlorophyll in the reaction centre, rather than passing on the excitation energy to a neighbouring pigment, an electron is transferred instead, resulting in the first charge separation. The "particular" reaction centre chlorophyll of the last sentence is known as the primary electron donor.

This photochemical reaction forms a pair of oppositely charged radicals: a highly reducing anion radical and a highly oxidising cation radical. A series of rapid electron transfer reactions occurs, out from the anion radical and in to the cation radical. Each of these reactions involves a decrease in the standard free energy and an increase in the distance between the charged radicals. This results in the formation of a series of radical pairs which are successively more stable. Similar events occur in all types of photosynthetic reaction centres (reviewed in [2] and see Figs. 1 and 5).

In Type I reaction centres (i.e. those from green sulfur bacteria, heliobacteria and Photosystem I from cyanobacteria), electrons are transferred through the protein and across the membrane, one by one from a soluble 1-electron donor to a soluble 1-electron acceptor. Photosystem I, for example, is a plastocyanin/ferredoxin photo-oxidoreductase, where plastocyanin, the electron donor, and ferredoxin, the electron acceptor, are both soluble, 1-electron redox carriers (reviewed in [3]).

Type II reaction centres (e.g. those from purple bacteria, Chloroflexi and Photosystem II (PSII) from cyanobacteria and chloroplasts),

Abbreviations: (B)Chl, (Bacterio)Chlorophyll; (B)Ph, (bacterio)Pheophytin; Cyt, Cytochrome; EPR, Electron Paramagnetic Resonance; DCMU, 3-3,4-Dichlorophenyl-1,1-dimethylurea; FTIR, Fourier Transformed Infra-Red; PSII, Photosystem II; Q, Quinone

☆ This article is part of a Special Issue entitled: Photosystem II.

* Corresponding author at: Molecular Biosciences, Biochemistry Building, Imperial College, London SW7 2AZ UK. Tel.: +44 207 5945329.
E-mail addresses: a.rutherford@imperial.ac.uk, alfred.rutherford@cea.fr (A.W. Rutherford).

0005-2728/$ – see front matter © 2011 Elsevier B.V. All rights reserved.
doi:10.1016/j.bbabio.2011.07.012

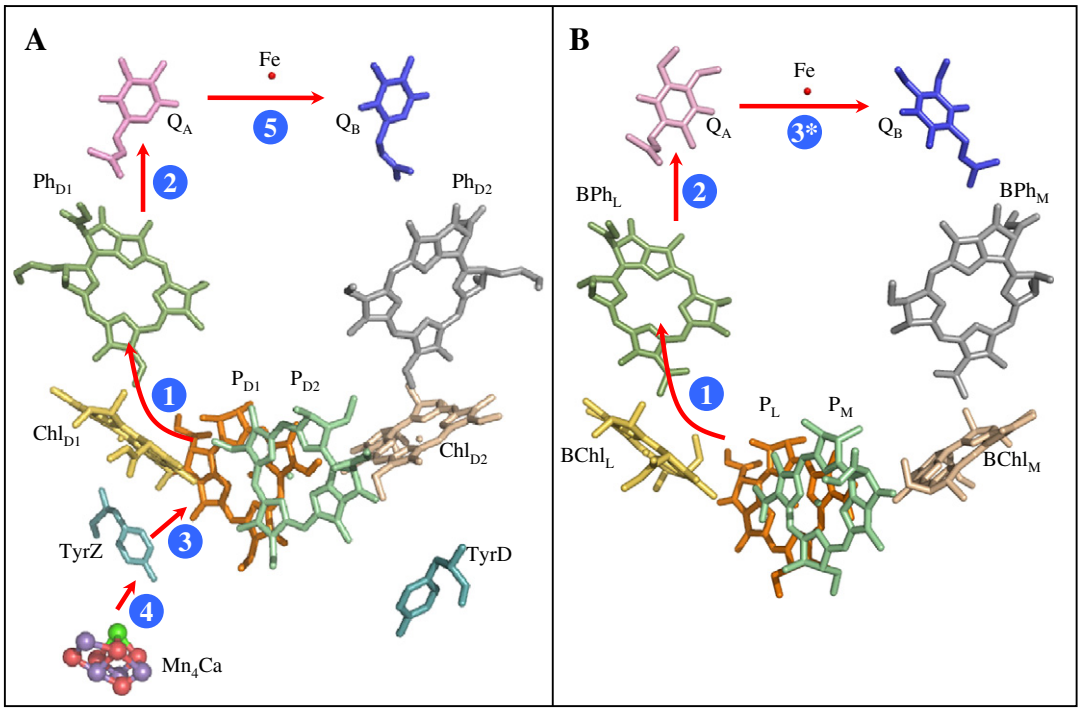

Fig. 1. A simplified scheme of charge separation and electron transfer events in (A) PSII and (B) the purple bacterial reaction centre. Red arrows represent electron transfer steps and the blue numbered circles the order of steps. Step 1 is shown in more detail in Fig. 2. The cofactors are labelled to make the comparison easier, using one of the conventions common in PSII research: i.e. with the central pigments called P, Chl and Ph (standing for Pair of chlorophylls, monomeric Chlorophyll and Pheophytin). These are then given a subscript that attributes them to the protein subunit that provides their main site, in PSII this is D1 and D2, in purple bacteria these are L and M. In the bacterial reaction centre, where the pigments are bacteriochlorophyll or bacteriopheophytin, this is indicated as BChl or BPh. The location of the cation radical after step 1 is mainly P_{D1} in PSII, while it is shared over P_L and P_M in purple bacteria. Step 3* in the purple bacteria bears the asterisk in order to indicate that it is not always the third step since conditions do arise in which electron donation from Cyt *c* heme to the cation on the P_LP_M pair, P^+, can be more rapid than the Q_A to Q_B electron transfer step. Similar qualifications can be given for some of the steps in PSII (see text), notably for steps 4 and 5, but the order is correct as drawn at least for the first charge separation from a dark-adapted and fully functional PSII. The figure was made using the structures for PSII (PDB ID: 3ARC) from the cyanobacterium *Thermosynechococcus vulcanus* and for the purple bacterial reaction centre (PDB ID: 3I4D) from *Rhodobacter sphaeroides*.

are more complicated. In all cases quinone is the final electron acceptor, and the fully reduced quinone, hydroquinone (QH_2), is released into the membrane. Quinone however is a 2-electron acceptor and, given the univalence (1 electron per photon) of the photochemistry, it is expected to undergo two sequential 1-electron reduction steps along with the associated protonation reactions, before its reduction is complete. In Type II reaction centres, the source of electrons varies. Purple bacteria have 1-electron donors, either cytochrome (Cyt) *c*2 or a bound tetraheme cytochrome, which is reduced either by Cyt *c*2 or by the high potential iron–sulphur protein, HiPIP [4,5]. PSII on the other hand takes electrons from a pair of water molecules: a 4-electron donor system (reviewed in [6,7]).

2. Photosystem II: introduction

PSII is a water/plastoquinone photo-oxidoreductase. With its 2-electron chemistry on one side and its 4-electron chemistry on the other, it is the most complicated of the reaction centres. PSII is also special for other reasons.

When PSII first evolved in the ancestors of cyanobacteria, its water oxidising activity led to radical changes both at the geological and biological level. The availability of water as an electron source allowed photosynthetic species to colonise most of the planet. Photosynthetic water oxidation put the O_2 into the atmosphere and the biosphere. This allowed respiration with O_2 as the electron acceptor, a much more efficient way of burning sugar than anaerobic processes (e.g. fermentation). This improvement in efficiency was a critical factor in the development of multicellular life. In addition, the O_2 in the upper atmosphere was converted into ozone (O_3) by UV-light. The ozone layer that was formed then screened out the UV and allowed life to colonise the surface of the planet [8,9].

Our understanding of PSII has been built on comparative work with the simpler purple bacterial reaction centre [10–12], which thus far has been the best-studied reaction centre (Fig. 1 B). With the general acceptance of the intrinsic similarities between the two types of reaction centres, there is a tendency to consider PSII as a chlorophyll-containing purple bacterial reaction centre "with a bunch of Mn ions stuck on the base" [13] (or the top, if you are from the bacterial world). While this can be a useful simplification, decades of comparative work have identified many features in the PSII reaction centre that are different from those in the purple bacterial reaction centre. This review focuses on some of these differences.

3. Charge separation in purple bacteria reaction centres

In the purple bacterial reaction centre the primary reactions occur as follows [14] (see Fig. 1 B). When the excitation arrives at the reaction centre bacteriochlorophylls, either directly by light absorption or by energy transfer from photoexcited antenna pigments, it becomes localised on the species (pigment) with lowest energy excited state, i.e. the longest wavelength pigment, a special pair of bacteriochlorophylls. This special pair of bacteriochlorophylls is designated P, for pigment, with *P being the excited state. Often P is followed by a number (e.g. P870), which indicates the wavelength of the bleaching when the system absorbs light; given that this varies from species to species, we will simplify to P. The designation "special pair" is used rather than dimer because they are not true chemical dimers [15].

The special pair of bacteriochlorophylls, P, which is made up of P_L and P_M are relatively strongly coupled (500 to 1000 cm^{-1}) compared to the coupling between the other pigments in the reaction centre [14]. For example, the electronic couplings between the special pair and the adjacent bacteriochlorophylls on the L and M subunits are

around 100 cm^{-1} [16]. These components (designated $BChl_L$ and $BChl_M$), are considered to be monomers. The strong coupling between P_L and P_M is responsible for the shift to longer wavelength of the absorption of P (of the two resulting exciton states, the low energy, long wavelength state dominates: it has nearly all the oscillator strength).

A few picoseconds after formation of *P, the $P^+BPh_L^-$ state is formed, where BPh_L is the bacteriopheophytin of the L subunit [17,18], (Fig. 1 B step 1). This state was clearly detected in the early ultrafast experiments, however it turned out that the intervening momomeric $BChl_L$ (for a while erroneously designated an "accessory" or "voyeur" pigment) was in fact the true primary acceptor, with the first charge separation, $P^+BChl_L^-$, occurring in 3 ps (Fig. 2 step 1a). This pair is stabilised by transfer of the electron from $BChl_L^-$ to BPh_L. This step is very rapid (1 ps), which was why the $BChl_L^-$ state was so difficult to detect [19].

It was subsequently shown that when excited directly, charge separation could be triggered from $*BChl_L$, resulting in the ultra-rapid formation of $BChl_L^+BPh_L^-$. Because of the localisation of the excitation on the long wavelength P, the slower charge separation from *P (as described above) dominates under normal circumstances. These observations however led van Brederode and van Grondelle [20] to suggest that the primary charge separation in PSII could occur from $*Chl_{D1}$ (Fig. 2A), in accordance with the earlier suggestions based on the unexpected location of the radical-pair recombination triplet on Chl_{D1} in PSII [21–23].

After formation of the $P^+BPh_L^-$ state, the next stabilisation step occurs in a few hundred picoseconds, with an electron being transferred from BPh_L^- to Q_A (a bound ubiquinone) [17,18,24]. This stabilisation step comes at the cost of a significant amount of energy, in the range of 0.6 eV (reviewed in [14]).

P^+ is stabilised by a change in the protein involving a near-by tyrosine [25,26]. A time-resolved Laue diffraction study, showed that the Tyr162 on the L subunit moved 1.3 Å closer to the special pair in less than 3 ms after the formation of P^+ [26]. It was suggested that this represented the P^+-induced deprotonation of the tyrosine, with the proton shipped off to the protein surface. This probably contributes to the stabilisation of the $P^+Q_A^-$ state that is frozen-in when reaction centres are frozen under illumination [27].

The $P^+Q_A^-$ state in most species is stabilised by electron donation from the tetraheme cytochrome that makes up the fourth subunit of the reaction centre [28] or by direct donation from Cyt *c*2 in those species lacking the tetraheme. The electron on Q_A^- is transferred to Q_B in around 100 μs, or to Q_B^- (when present) with $t_{1/2}$ values of around 1 ms. The doubly reduced and protonated Q_BH_2 is exchangeable and is replaced by a quinone from the pool in the membrane. This exchange process takes place in about 10 ms (reviewed in [29,30]).

The Cyt *c*2/ubiquinone photo-oxidoreductase function of the purple bacterial reaction centre is complete after two photochemical turnovers. Much of the complexity is in the proton-coupled electron transfer associated with the 2-electron quinone chemistry and that is described in more detail in a later section.

4. Charge separation in Photosystem II

In PSII the overall picture of charge separation is similar to that in the purple bacterial reaction centre (reviewed in [31], see Fig. 1). There are however differences. The first difference is at the level of the very first events (Fig. 2). Various models exist, and the picture is not completely clear but here we present one model that has had a good deal of support (reviewed in [32,33]).

The structural counterparts to the special pair P (P_L and P_M) in the purple bacterial reaction centre are designated P_{D1} and P_{D2} in PSII. The electronic coupling between these two chlorophylls is estimated to be between 85 cm^{-1} and 150 cm^{-1} [34–38], with the higher values coming from the more recent studies on more native PSII preparations and with the benefit of more detailed structural information. This coupling is weak compared to the situation in the bacterial reaction centre (500–1000 cm^{-1}) [14]. It has long been thought that the intrinsic electronic and structural properties of chlorophyll compared to bacteriochlorophyll could contribute to the weaker coupling. Chlorophyll, with its aromaticity shared over a greater area (ring II is aromatic in chlorophyll, see Fig. 3), might have a somewhat weaker electronic coupling in a chlorophyll special pair with the exact geometry of the bacteriochlorophyll special pair (see Fig. 3). More recent experimental work however has shown that the geometry of the $P_{D1}P_{D2}$ pair is not identical to the special pair in the purple bacteria reaction centre. $P_{D1}P_{D2}$ are rotated in the plane of their rings relative to each other and this effect is asymmetrical with P_{D2} being slightly shifted upwards into the membrane [38–40]. Short range interactions are the main determinants of the level of electronic coupling in these systems [41], so the rotation of the rings will have marked effects in orbital overlap, e.g. the almost perfect overlap (or "eclipse") of the aromatic ring I in the purple bacterial P_L/P_M pair is lost in PSII due to the rotation of the P_{D2} relative to P_{D1} in PSII (see Fig. 3) [39].

The weak coupling between P_{D1} and P_{D2} (85–150 cm^{-1}) is not much greater than between the other four central pigments (the individual couplings of P_{D1} and P_{D2} with Chl_{D1} and Chl_{D2}, and the

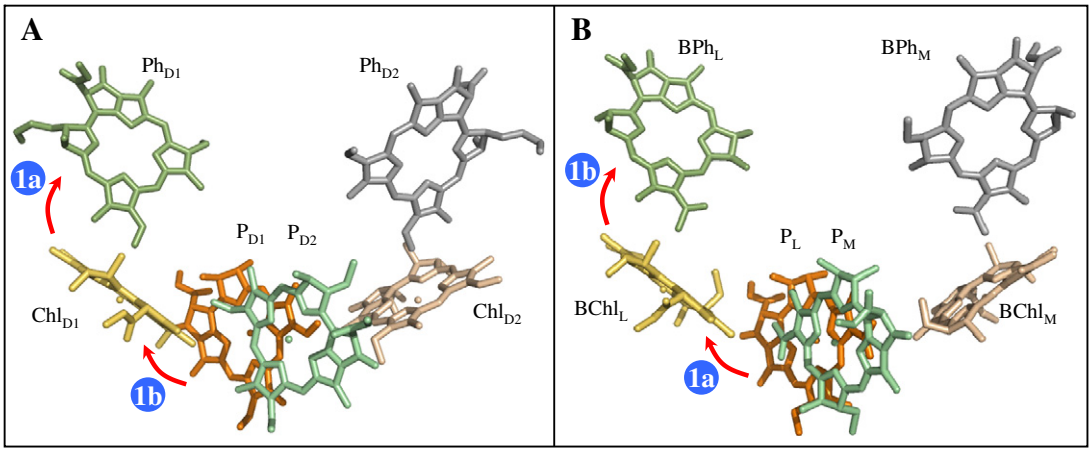

Fig. 2. Differences in the first steps of charge separation in (A) PSII compared to (B) purple bacterial reaction centre. The arrows show the electron transfer steps and the numbers in the blue circles the order of the steps with 1a representing the initial electron transfer step and 1b the subsequent step. Note that these are different in the two different kinds of reaction centre. For PSII the scheme shows what is considered to be the reaction sequence in the dominant fraction of centres. In PSII other primary charge separation reactions and electron transfer sequences are thought to occur in smaller fractions of centres, and these include a sequence comparable to that occurring in purple bacterial reaction centres.

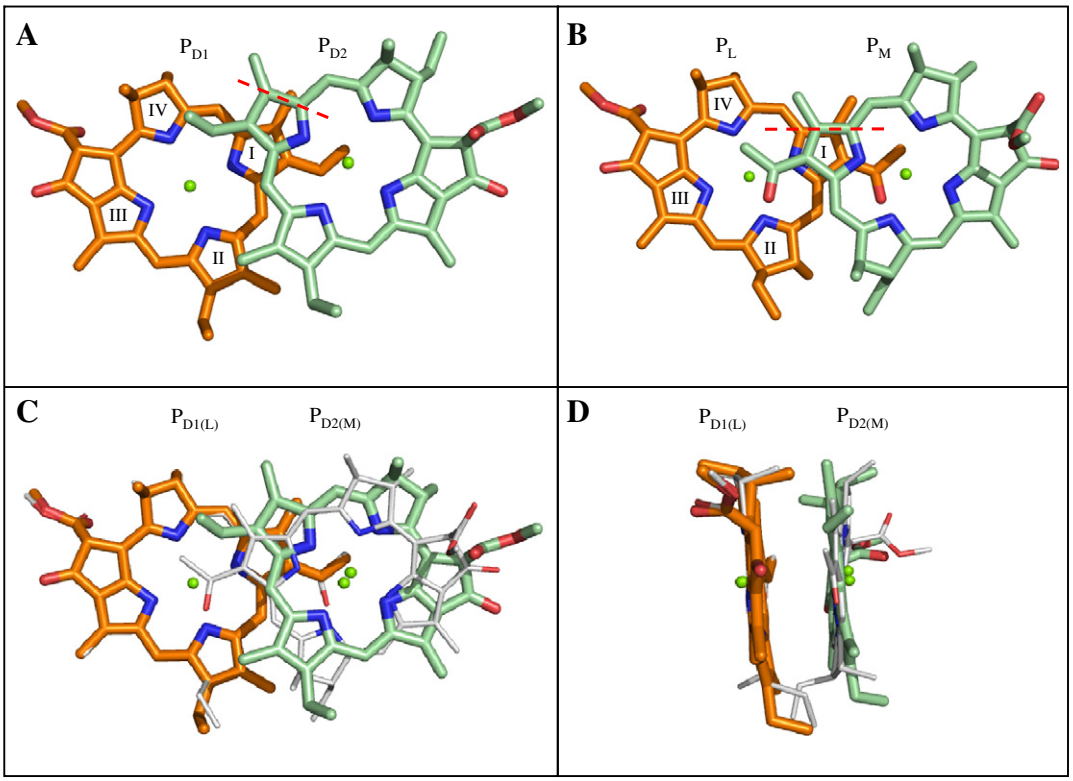

Fig. 3. Structural comparison of (A) the $P_{D1}P_{D2}$ chlorophyll pair of PSII and (B) the bacteriochlorophyll pair P_LP_M from the purple bacterial reaction centre. The roman numerals determine the ring number in the (bacterio)cholorphyll. Notice the break in symmetry of P_{D2} relative to P_{D1}, where the ring I of P_{D2} does not overlap with that of P_{D1}, in contrast to the situation in the purple bacterial reaction centre. In panel (C) and (D), P_{D1} (thick orange sticks) and P_{D2} (thick green sticks) have been overlapped with P_L and P_M (thin white sticks) to further illustrate the differences. In panel (D) the overlapped pairs are rotated 90°, notice that the distance from P_{D1} to P_{D2} is virtually the same in the P_L and P_M pair.

couplings of Chl_{D1} and Chl_{D2} with the two pheophytins are around 50 cm^{-1}). Based on the magnitude of couplings in the bacterial reaction centre (where the coupling in the special pair between P_L and P_M is 500–1000 cm^{-1} and the coupling between P and the "monomeric" chlorophylls, $BChl_L$ and $BChl_M$ is 100 cm^{-1} [37,38]), P_{D1} and P_{D2} in PSII might be considered as monomers. An alternative view is that the 6 weakly coupled pigments in PSII (the 4 chlorophylls plus the 2 pheophytins) represent a multimer [37]. The most recent model however sees P_{D1} and P_{D2} as a weakly coupled pair, with its geometry giving rise to a coupling with a strength and character that is unique among interactions between the pigments of PSII [38,42].

The description of the $P_{D1}P_{D2}$ pair is important when it comes to assigning the changes in absorption that occur when charge separation takes place. However, the important issue here is that the coupling of the $P_{D1}P_{D2}$ pair does not result in the generation of a long-wavelength energy trap. Indeed the absorption spectra of all the chlorophylls and both the pheophytins overlap to a large extent. This means that when the excitation arrives at the PSII reaction centre, it does not localise on one specific pigment. The ambient thermal energy is enough to ensure that the excitation could be on any of the four central chlorophyll and also the two pheophytins. What then occurs is not a single, easy to follow series of reactions, with an initial charge separation reaction followed by a specific series of stabilisation reactions, like that occurring in purple bacterial reaction centres. Instead, in PSII a slew of different charge separations occurs in the first few picoseconds after excitation, potentially involving, $P_{D1}^+P_{D2}^-$, $P_{D1}^+Chl_{D1}^-$, $Chl_{D1}^+Ph_{D1}^-$, etc. [32].

A short time after the initial charge separation reaction (a few tens of picoseconds), electron transfers take place producing the charge pair, $P_{D1}^+Ph_{D1}^-$. This secondary radical pair corresponds to the second radical pair, $P_L^+BPh_L^-$, in the bacterial reaction centre (see Fig. 2).

Overall then, while the first step is different in PSII compared to the bacterial reaction centre, after a few tens of picoseconds, things have lined up again, with the secondary radical pairs being comparable. There is however an important difference between the two secondary radical pairs: the cation radical is delocalised over both bacteriochlorophylls of the special pair, P^+, while in PSII the cation is mainly localised on P_{D1} [43,44].

The often used designation "$P680^+$" (i.e. the pigment bleached at 680 nm) corresponds to P_{D1}^+ and while *it is not the* "*primary*" *electron donor* in most centres, it is the relatively stable location of the cation after the first tens of picoseconds [45].

It is worth noting that a primary charge pair more comparable to that in bacteria (i.e. $P_{D1}^+Chl_{D1}^-$) probably is formed in a fraction of centres. This might be favoured by selective illumination [46] into a very weak (low oscillator strength) long wavelength absorption [47] that may be a charge transfer state from the $P_{D1}P_{D2}$ pair [46,47].

Although the chlorophylls and pheophytins in PSII have overlapping absorptions, they are not identical. Identifying the contributions of each pigment to specific absorptions has been tricky to say the least (compare [38] and [46] for current contrasting assignments). To add to the problem the absorption characteristics are affected by the isolation procedures particularly in the smallest (and most used) "D1D2" preps. In the most convincing model, the longest wavelength pigment in PSII is thought to be the Chl_{D1} [38,42,48]. This should favour the localisation of the excitation on this pigment and the distribution of primary charge pairs is expected to favour $Chl_{D1}^+Ph_{D1}^-$. Thus for some years Chl_{D1} has been considered as the "primary electron donor" or at least the main one [22,23,31,32,38,43,44].

At low temperature, Chl_{D1} is the site of the triplet state [22,23,49] formed from $P_{D1}^+Ph_{D1}^-$ recombination. This contrasts to the situation in other reaction centres, where it is localised on the special pair chlorophylls [50–54]. This observation was not only the first experimental evidence for the existence of a Chl_{D1} that was the structural counterpart to $BChl_L$ in purple bacteria [22] but also the basis for the suggestion that this pigment was the "primary donor" of PSII [21–23]. The first of these suggestions was confirmed by the crystal structures

of PSII [55–57] and the second was supported by spectroscopic studies on mutants [49], ultrafast kinetic measurements [43,44] and calculations [48].

When $P_{D1}^{+}Ph_{D1}^{-}$ charge recombination occurs in a centre in which Q_A^- is present, the triplet state formed, $^3Chl_{D1}$, has a lifetime that is more than a hundred times faster than the typical chlorophyll triplet [58,59]. The much longer 2 ms range triplet lifetime at 20 K, typical of other chlorophyll triplets, was seen when Q_A was double reduced or absent [58–60]. No significant quenching by carotenoid was seen under these conditions. (A recent report of chlorophyll triplet quenching by β-carotene in the presence of Q_A^- [61] contradicts earlier studies and while intriguing seems to require more quantitation and comparative studies at similar temperatures before the earlier work is seriously questioned.) Despite earlier suggestions [60] this effect was clearly not related to an electrostatic effect on yields/lifetimes of the radical pair or triplet. Nor was it related to a magnetic effect of the Fe [64]. It was suggested that the abnormally short lifetime of the triplet was due to an electron transfer quenching from Q_A^- to the triplet state [58]. It was proposed that this occurred through migration of the triplet to the Ph_{D1}, which is adjacent to the Q_A^- [58], see also [63,64]. It was further suggested that the location of the triplet on Chl_{D1}, adjacent to the Ph_{D1}, favoured this mechanism and could be considered an important protective mechanism [64]: an idea that was later championed by Noguchi [65] (see [66] for more recent kinetic studies of this problem).

At low temperature Chl_{D1} should act as a more localised trap for the excitation, and charge separation between Chl_{D1} and the adjacent Ph_{D1} may represent the dominant reaction. However, two different charge separation pathways have been suggested to occur at cryogenic temperatures in D1D2 core preparations [67]; with $Chl_{D1}^{+}Ph^{-}$ in some centres and $P_{D1}^{+}P_{D2}^{-}$ (and then $P_{D1}^{+}Chl_{D1}^{-}$) in other centres formed prior to formation of the secondary pair $P_{D1}^{+}Ph_{D1}^{-}$. This presumably reflects the freezing-in of structural disorder which gives two distinguishable excitation traps and their different charge separation sequences. These charge separation sequences were suggested to be present at physiological temperatures and in more intact PSII [67].

The possibility that different primary charge pairs may be formed depending on minor changes in structure and environment may be significant in terms of function. The final location of the cation is the most relevant factor for functional effects. If, for example, the cation were located on Chl_{D2} under conditions of high photon flux, it would result in efficient electron transfer from the β-carotene/Cyt *b*559/$ChlZ_{D2}$ side-pathway (reviewed in [68,69] see below and Fig. 4, blue arrows).

The secondary radical pair, $P_{D1}^{+}Ph_{D1}^{-}$, is stabilised by electron transfer to Q_A in 400 ps [70] with a significant energy loss, [31,71,72] (see Fig. 5). This contributes to stabilising the $P_{D1}^{+}Q_A^{-}$ radical pair (Fig. 1A step 2), much as seen with the purple bacterial reaction centre [14]. P_{D1}^{+} is highly oxidising (estimates range from 1.2 to 1.4 V) [73–75] and it is able to take an electron from tyrosine 160 of D1 (step 3 in Fig. 1A). This tyrosine is designated TyrZ. The oxidation of TyrZ is accompanied by its deprotonation, which is mediated by an H-bond to the imidazole of histidine 190 of D1 [76,77]. The electron transfer step from TyrZ to P_{D1}^{+} occurs with a $t_{1/2}$ of 50 ns for dark adapted PSII (i.e. when the S_1 state is present). The neutral tyrosyl radical, $TyrZ^{\bullet}$, is able to oxidise the Mn_4Ca cluster (step 4 in Fig. 1A), the active site for water oxidation. Starting from the dark-adapted state (S_1), electron donation to $TyrZ^{\bullet}$ has a $t_{1/2}$ of around 55 μs [78].

The necessity to specify the "S state" when giving the rates of P_{D1}^{+} and $TyrZ^{\bullet}$ reduction, reflects the fact that the rates vary depending on the S state (see [79] for a compilation of rates reported in the literature). The main factor responsible for this is that the S_1 to S_2 step results in the accumulation of a positive charge on or close to the cluster [7]. The electrostatic effect of this charge slows down electron transfer. Thus when S_2 and S_3 are present, this extra charge is present and P_{D1}^{+} reduction slows from 50 ns to 250 ns, while $TyrZ^{\bullet}$ reduction slows from 55 μs to 290 μs [78]. For the S_3 state, $TyrZ^{\bullet}$ reduction is even slower, around 1 ms, this is the rate-limiting step of water oxidation [7].

On the electron acceptor side, the electron on Q_A^- is transferred to Q_B (or Q_B^- when present), see Fig. 1A step 5. This occurs in 0.2–0.4 ms forming Q_B^- (or 0.8 ms forming Q_BH_2) [80,81]. When Q_BH_2 is formed, it is released from the site and is replaced by a quinone from the pool in the membrane.

In the previous paragraph, the necessity to mention electron transfer on the first flash from Q_A^- to both Q_B and Q_B^- reflects the heterogeneity in a dark adapted PSII sample [82,83]. In the light, prior to dark adaptation, it is assumed that there are equal populations of Q_B and Q_B^- and of each of the long-lived S states (S_0, S_1, S_2, S_3). Q_B^- decays by recombination only in centres where S_2 and S_3 are present [83]. When S_0 and S_1 are present Q_B^- cannot recombine and is stable in the dark for many hours.

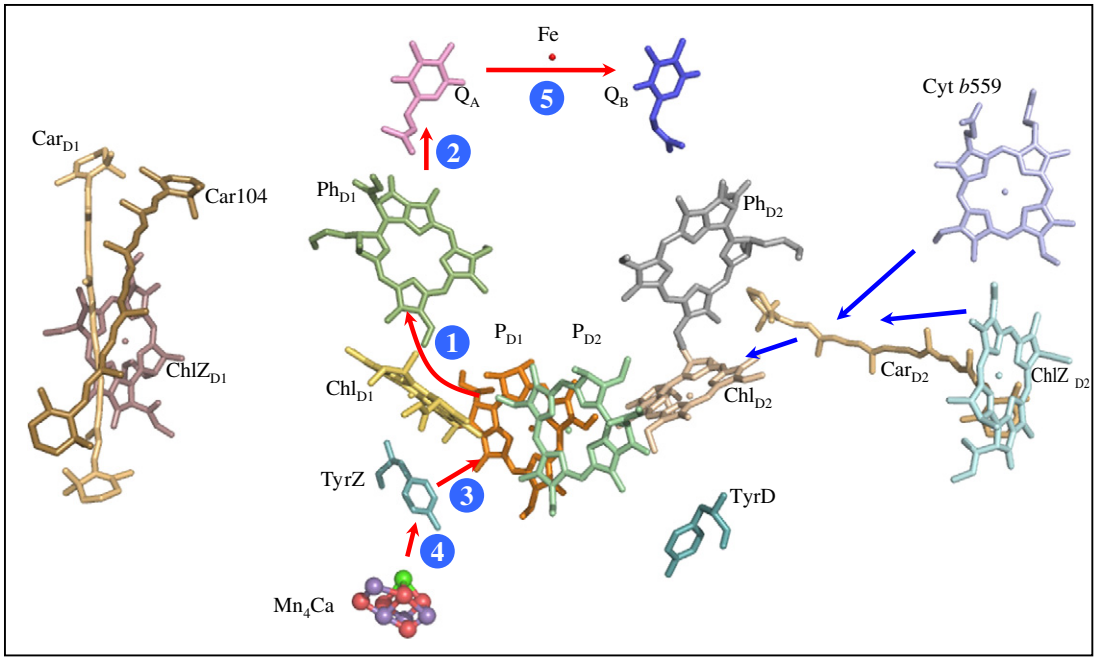

Fig. 4. Electron transfer side-pathway of PSII. Red arrows represent the main events of charge separation while the blue arrows indicate the low quantum yield, side-pathway electron transfer reactions.

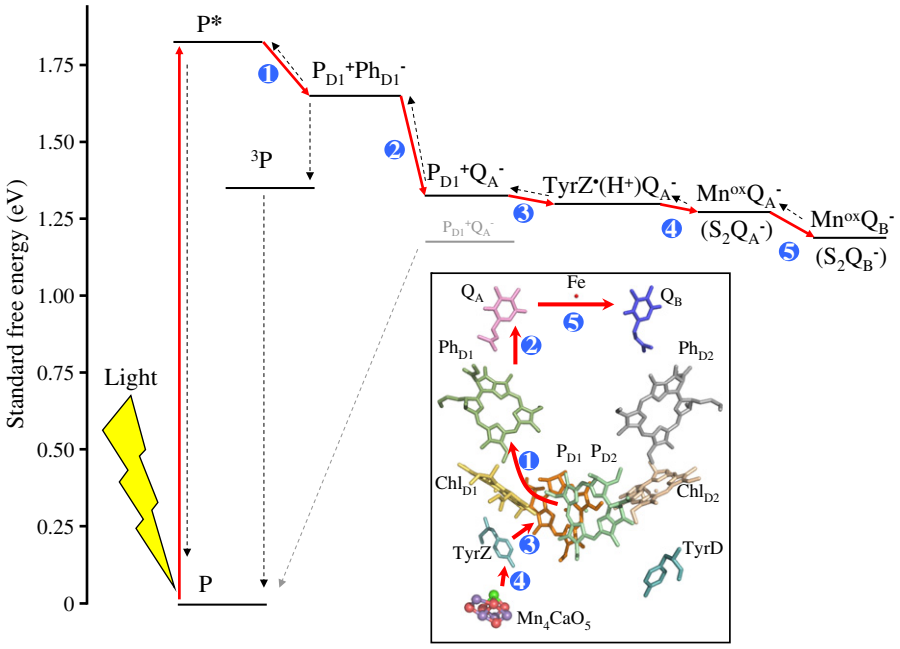

Fig. 5. An energy scheme of the electron transfer steps in PSII occurring after the absorption of one red photon and assuming that all centres are in the dark adapted stable state, S_1. The inset shows the PSII cofactors involved in charge separation and the numbers in the blue circles indicate the order of the reactions. After absorption of the red photon the first excited singlet state is 1.83 eV above the ground state. Excitation of the core pigments P, which are all weakly coupled, leads to the formation of $P_{D1}^+Ph_{D1}^-$ as the first easily identifiable radical pair, this is designated step 1. In the text and in Figure 2 the more complex aspects of this first step are described in detail. After each subsequent step some energy is lost, with a major loss after the formation of the $P_{D1}^+Q_A^-$ radical pair. P_{D1}^+ is able to oxidise the redox active TyrZ, forming the neutral radical $TyrZ^{\bullet}$ with proton transfer to the near-by His190 (step 3). The $TyrZ^{\bullet}$ oxidises the Mn_4Ca cluster by one electron forming the S_2 state (step 4). Finally, electron transfer from Q_A^- to Q_B occurs (step 5). The absorption of 4 photons is necessary to complete a cycle of water oxidation and the reduction of two plastoquinone molecules. Back reactions are shown as broken lines. The triplet state, ^3P, is formed from a triplet form of $P_{D1}^+Ph_{D1}^-$, which is mainly formed by the back reaction but for simplicity this is not distinguished from the singlet radical pair in the figure. The back reaction from the high potential form of Q_A– (in inactive centres) is shown in grey (see section 9.1).

Overall, when a photon is absorbed by PSII, within 1 ms the Mn_4Ca cluster is oxidised by 1 electron and the quinone is reduced by 1 electron. This occurs with a quantum yield close to 90% and more than half of the energy of the red photon [6] is conserved in the charge separated state. From a dark-adapted state, in which the majority of the centres are in the S_1Q_B state, the $S_2Q_B^-$ state is formed. This state is stable in the tens of seconds and decays with a $t_{1/2}$ of around 30 s at 20 °C by charge recombination [83,84].

In order to complete the reactions stated in its job description as a plastoquinone/water photo-oxidoreductase, PSII must undergo a second photochemical charge separation before the first charge pair decays in order to reduce the quinone fully and a total of four turnovers are required to remove 4 electrons from 2 molecules of water [7].

5. What makes "P680$^+$" such a strong oxidant and how did it evolve?

P_{D1}^+ ($P680^+$) has a potential between 1.2 and 1.4 V. This is 0.5 V higher than the potential of isolated chlorophyll in solvent and 0.7–0.9 V more oxidising than P^+ in purple bacterial reaction centres. How the protein imposes this high potential has been a long-standing question. Here we will discuss briefly what factors contribute to this very high potential compared to P^+ in bacterial reaction centres.

Based on X-ray crystallographic data the redox potentials of the cofactors have been calculated and the various electrostatic influences deduced [85]:

1) P_{D1}^+ is a chlorophyll and is consequently 160 mV more oxidising than if it were a bacteriochlorophyll [86].
2) The cation is localised mainly on P_{D1} and does not seem to be shared over two pigments. This contributes 140 mV, estimated for a chlorophyll pair from density functional calculations [87].
3) There are several specific electrostatic effects that accumulate to make P_{D1}^+ more oxidising [85]. i) The Mn_4Ca cluster is bound in its vicinity and this is estimated to increase the potential by 200 mV. ii) The accumulated affect of dipoles from the backbones of the trans-membrane helices contributes 150 mV compared to the potential of P^+ in the bacterial special pair. iii) Somewhat surprisingly, the effect of amino acid side chains is to *down-shift* the potential of P_{D1} by −135 mV. This compensates the asymmetric effect of the Mn_4Ca cluster on the potentials of the core pigments. This maybe important since it presumably contributes to tuning the potential of P_{D1}^+ to make it less oxidising than the neighbouring chlorophylls (P_{D2}, Chl_{D1} and Chl_{D2}) and thus allows the cation radical to be localised specifically on P_{D1}. iv) Structural differences in the cd parallel helix (which is longer in PSII, lacks a ligand to Chl_{D1}, and bears the TyrZ H-bond partner, His190, and the Mn ligand, Glu189) shift the potential up by around 100 mV. v) Another 200 mV up-shift is imposed by the atomic charges and protein dielectric volume of the peripheral proteins in PSII that are absent in the purple bacterial reaction centre.

So to summarise, the oxidising nature of the cation of PSII is mainly due to it being a chlorophyll monomer in a "big fat" multiprotein complex in which it is in the right position to experience the large effect from the backbone dipoles from the trans-membrane helices. This already buys 650 mV more oxidising power than P^+ in bacterial reaction centres and up to 500 mV more than chlorophyll in solvent. This change could have occurred with a small number of mutations in a homodimeric ancestor provided the homodimeric ancestor was a big fat protein. This fits with the idea that PSII evolved from a chlorophyll-containing Type I reaction centre ancestor (rather than the small, 2 x 5 trans-membrane helices, purple bacterial-type reaction centre) and that its high oxidising power evolved in a homodimeric reaction centre [23,88]. It is worth considering the possibility that the splitting of the 11-helices reaction centre gene of Type I reaction centres into the 5-helices Type II reaction centre plus the 6-helices core antenna proteins found in PSII, could have been linked to a change in the environment of P. Irrespective of whether it occurred in Type I (2×11 helices) or Type II (with $2\times5+6$ helices) reaction centres, the

simultaneous uncoupling of the chlorophyll pair and shift in position of its histidine ligand along the helix (thereby picking up the effect of backbone dipoles described in [86]) would have resulted in a sudden jump in its potential. The subsequent binding of Mn would then push up the potential even further, high enough for water oxidation. For more details relevant to this view see [23] and [88]. For other views and other aspects of PSII evolution see [89,90].

Having discussed all the factors that make P_{D1}^{+} so oxidising, it is worth reiterating the point that, in order for it to be the main location of the cation radical, all the other near-by chlorophylls (i.e. P_{D2}, Chl_{D1} and Chl_{D2}) must have even higher potentials (or they would be oxidised by P_{D1}). The main factors responsible for the high potential of P_{D1}, listed above, do the same for its neighbouring pigments give or take some fine tuning (see [85]). In the putative homodimeric water-oxidising ancestral protein, the redox potentials of P_{D1} and P_{D2} would by definition have been the same.

6. Similarities between PSII and purple bacterial reaction centres: a short history

It is well accepted that the purple bacterial reaction centre is similar to that of PSII. In the 1970s, however, this was far from clear, although some signs were there in the literature. While chlorophyll/bacteriochlorophyll photo-oxidation in the primary reaction was common to all reaction centres, quinone chemistry seemed to be in common only to PSII and purple bacterial reaction centres [91,92]. In both systems, the "primary acceptors" were shown to be quinones (Q_A) [92–94]. The secondary acceptors were also shown to be quinones in both types of reaction centres with the same period-of-two behaviour with flash number, indicating sequential, 1-electron reduction steps of a 2-electron accepting species: Q_B [95–98].

The absorption difference spectrum for Q_A/Q_A^- showed a band shift at 550 nm, which was interpreted as a pheophytin close to the Q_A^- anion in the heart of the reaction centre [92]. Meanwhile, in the purple bacterial reaction centre, bacteriopheophytin was demonstrated to be an electron acceptor functioning prior to Q_A [17,18]. Having been involved in the study of bacteriopheophytin reduction in purple bacteria, Klimov and coworkers [99] tried the same thing with PSII and indeed found Ph^- photo-accumulation at low potential. As the authors pointed out, this steady state approach was not definitive proof that the pheophytin was an early acceptor in PSII, it was nevertheless an attractive option.

In the early 80s several discoveries were made that argued strongly in favour of structural and functional similarities. A "split radical" EPR signal arising from the Ph^- was reported [100]. This was very similar to that from BPh_L^- interacting magnetically with $Q_A^-Fe^{2+}$ in bacterial reaction centres [101]. The same magnetic interaction appeared to be present in PSII and thus the presence of a (not detected) semiquinone–iron complex was implied [100]. Experiments aimed at removing and replacing the iron were taken as support for this suggestion [100]. A specific spin polarised triplet state was found in PSII [102] very similar to that in bacterial reaction centres [103,104], with a polarisation pattern that was a finger print for radical pair recombination [105]. This state was lost when the Ph^- was reduced, showing that pheophytin was involved in an early radical pair in PSII [102,106]. Kinetic studies also indicated that the Ph^- was formed as part of the radical pair when Q_A was reduced [107].

The typical EPR signals from the semiquinone–iron complex were harder to find despite the indirect evidence for its presence from the report of the split Ph^- EPR signals [100]. Early reports were not very convincing [108,109], but in the light of the data from the split EPR signal from Ph^-, these early reports were given the benefit of the doubt. Later it was shown that Q_A^-Fe signals like those seen in purple bacteria are present in only a small fraction of (modified) centres unless formate is added [110]. Indeed "native" PSII exhibits a quite different EPR signal to that in most bacterial reaction centres [110,111]. This seems to arise from an important difference in the ligand environment of the iron: purple bacteria have glutamate as a ligand while PSII has bicarbonate [10,39,57,112,113] and this may exist as carbonate in the native system [114], see Fig. 6.

By the early 80s then, it was clear that both systems contained a (bacterio)chlorophyll primary electron donor, a (bacterio)pheophytin intermediate electron acceptor, followed by two quinone acceptors functioning in series; one of which was a 1-electron carrier and the other a 2-electron acceptor. These marked similarities were already a firm basis to argue for similar structures. However the similarities in the EPR signals from the semiquinone–iron complex (once treated with formate to obtain the same ligand environment [110]) indicated more than that. The precise distances and orientations required in order to get identical EPR signals from the weak electronic interaction between semiquinone and the high spin non-heme iron argued not just for simple similarity but for true structural homology. So by 1984 evidence existed indicating that PSII and purple bacterial reaction centres at a basic level had the same structure, at least at the level of the electron acceptor side [110,112].

When the first crystal structure of the purple bacterial reaction centre came out [115], it directly provided models for PSII. There followed a wave of studies, testing and extending the model, these included the following: i) amino acid sequence comparisons provided the folding models for D1 and D2 [10,116,117]. These were strongly supported by clustering of the Q_B site amino acids implicated in herbicide resistance [116] and by biochemical approaches [118]. ii) The isolation of a D1D2 reaction centre confirmed the idea that D1D2 were counterparts of L and M [119]. iii) The folding models of L and M were verified by site-directed mutagenesis [120,121]. iv) Detailed computer models of the transmembrane parts of D1 and D2 were built based on the bacterial reaction centre [122]. v) Extensive biophysical studies defined the distances and orientations of the cofactors and some of their protein environments (e.g. [123–127]). vi) Electron crystallography confirmed the 5 transmembrane helices within each of the core subunits D1 and D2 similar to the bacterial reaction centre [128]. Gradually improving X-ray crystallography at first mainly verified the established structural model [55,56] and put to rest some outstanding ambiguities [13]. The subsequent refined structures provided a vast quantity of detailed information that is still being mined to obtain improved understanding of the differences between the two kinds of reaction centres [40,57,129]. The recently published 1.9 Å model will take this up to another level of detail after resolving the position of every atom in the Mn_4Ca cluster and revealing the location of thousands of water molecules [39].

7. Evolution of Type II reaction centres: the quinone iron complex

Perhaps the biggest surprise from that first crystal structure of the purple bacterial reaction centre was that the reaction centre was a pseudo-heterodimer [115]. This was made up of L and M membrane-spanning subunits, with the relatively evenly spaced cofactors arranged in series to allow trans-membrane electron transfer in each symmetrical subunit. It was however quite clear from spectroscopic studies that just one side worked: only one bacteriopheophytin (BPh_L) underwent rapid transient reduction, while the other bacteriopheophytin could be reduced only very slowly and under special conditions, only one quinone (Q_A) acted as an acceptor from BPh_L and as a donor to a specialised 2-electron accepting Q_B. It seemed obvious then that the reaction centre had evolved from a true homodimer that had been able to do charge separation on both sides of the reaction centre.

It is possible to rationalise the evolutionary pressures that drove the change from an ancestral homodimeric reaction centre to the current heterodimeric reaction centres. These have been discussed elsewhere [23,88] (see also [90]) but will be reiterated here.

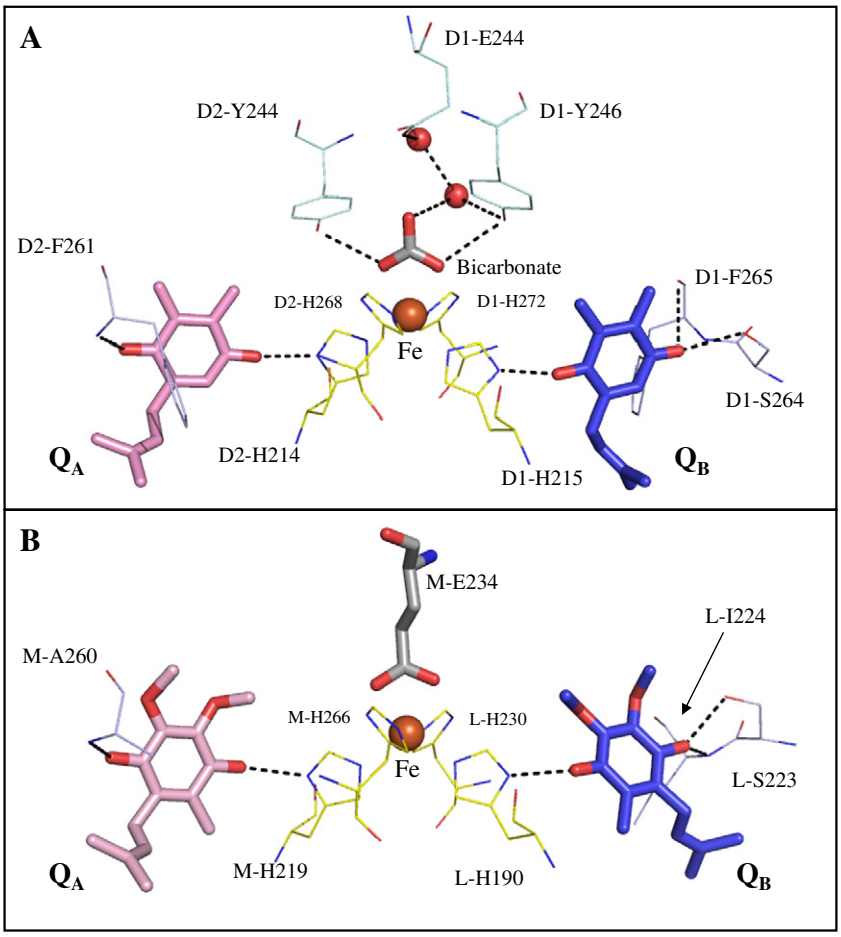

Fig. 6. Comparison of the Q_AFeQ_B electron acceptor complex in (A) PSII and (B) the purple bacterial reaction centre. The dotted lines represent H-bonds. In both figures Q_A is drawn in pink sticks while Q_B in blue, the yellow lines show the 4 coordinating histidines to the Fe, here drawn as an orange sphere. In panel (A), bicarbonate (grey sticks) serves as a bidentate ligand to the Fe of PSII; this is H-bonded to two symmetrical tyrosine residues (D2-Y244 and D1-Y246) and via water molecules to a glutamate residue (D1-E244), as visualised in the recent crystal structure at 1.9 Å by Umena et al. [39]. In contrast, the non-heme Fe of the bacterial reaction centre (B) is coordinated by a glutamate residue (M-E234).

The following assumptions are made concerning the properties of an ancestral homodimeric Type II reaction centre.

1) It was symmetric in structure and therefore in function.
2) Its function was the same as that of existing reaction centres: producing QH_2 in the membrane. For simplicity we shall not deal with the special features of the electron donor side here (see [88]).
3) The properties of the two quinones, (Q) had features of both Q_A and Q_B. Like Q_A, they could accept an electron from Ph^- and they could donate an electron laterally to a second quinone. Like Q_B^-, Q^- could accept an electron from another semiquinone, become protonated, form the hydroquinone and exchange with a quinone from the pool. In terms of binding properties then, we have to suppose that the quinones were neither tightly bound like Q_A (because exchangeability is a requirement for function), nor easily exchangeable (because it must be in place when the Ph^- is ready to donate). Thus the binding properties of the two quinones would likely be somewhere between those of Q_A and Q_B.
4) An important assumption is that once the semiquinone is formed, it is unable to act as an efficient electron acceptor from Ph^-. This assumption is based on the situation in existing reaction centres: there are no cases known in which the second reduction of quinone occurs from the Ph^- (or for that matter, Chl^-) in an efficient way. Q_A can undergo a light-driven second reduction but it is very slow and occurs with a very low quantum yield (see e.g. [60]). This is presumably due to a combination of electrostatic effects (Q_A^- destabilising the P^+Ph^- charge pair) and the exclusion of protons from the Q_A site. In the homodimer, protons had to be available but the requirement for proton binding during the reduction of Q^- would likely render the reaction slow compared to the P^+Ph^- back reaction. It is possible to imagine other scenarios in which the semiquinone in the homodimeric ancestor is protonated and yet remains bound in the site etc. In this evolutionary discussion, however, we use existing features as the first level of limitations for the arguments (see the section 9.7 below on Fe oxidation for another mechanism of quinone reduction that may be relevant to evolutionary thinking).

Given these characteristics for the ancestral homodimeric Type II reaction centre, we can now run through what might be expected upon charge separation, pointing out potential inefficiencies compared to the existing heterodimeric reaction centre.

1) The first excitation of the reaction centre would lead to charge separation and electron transfer occurring with an even chance on either side of the reaction centre. The first inefficiency is the possibility that the Ph^- would encounter an empty Q site due to the binding constant being lower than that of Q_A, because of the necessity for the quinone to be exchangeable. In the existing Q_B site, it is considered that Q_B and Q_BH_2 have similar binding constants (e.g. [29,30]. Even if Q were more tightly bound than QH_2 in the homodimer, it is unlikely that the occupation of the site would be 100% like the Q_A of today. If P^+Ph^- encountered an empty site, being relatively short-lived (in the time range of

around 100 ns), it is likely that it would recombine and that the energy would be lost.

2) In the majority of centres, Ph^- would encounter Q in the site and so P^+Q^- would be formed. The electron on Q^- could transfer laterally onto the second Q. Since the two quinones are identical, there would be no driving force for this and thus no additional stability would be associated. In existing reaction centres, the electron transfer step to Q_B is an additional stabilisation step. Furthermore, $P^+Q_B^-$ decays in a back-reaction via $P^+Q_A^-$, not through populating the Ph^- adjacent to Q_B^-; that is because the energy gap between Q_B^- and Ph_M is thought to be very big. Thus in the homodimeric reaction centre, the P^+Q^- state has a shorter back reaction pathway and would be less stable than $P^+Q_B^-$. This would likely result in more energy loss by charge recombination.
3) Assuming the P^+Q^- state is stabilised by electron donation to P^+, then P becomes available for a second excitation. If this occurs, as before, with an equal chance on either side of the reaction centre, then there is also an equal chance that the Ph^- will find itself confronted with a Q^-. As described in the assumptions above, it is likely that the energy would also be lost. It is possible that the presence of the Q^- could have an (electrostatic) influence on charge separation, favouring the side of the reaction centre without Q^-. Nevertheless, it seems reasonable to suggest that the risk of Ph^- encountering Q^- will still be a potential source of inefficiency in a homodimeric reaction centre.
4) When the second charge separation occurs on the side where Q rather than Q^- is present (i.e. in half the centres), then electron transfer to form Q^- is expected to occur, forming the Q^-Q^- state. Disproportionation then takes place forming Q and QH_2. The QH_2 is then released from the site and replaced by a new quinone from the pool. If however another charge separation takes place while this exchange process is occurring, then there is an even chance that Ph^- will encounter an empty Q site and thus that charge recombination will occur and the energy be lost.

All of these inefficiencies could have existed for a very long time, providing that competition for light was not a crucial evolutionary pressure. Indeed it has been suggested that water oxidation evolved in a homodimeric reaction centre [23,88]. (The presence of water oxidation in the homodimer could have constituted another important selection pressure for formation of a heterodimer [88] but that complication will not be dealt with here.) Based on the inefficiencies described above, when competition for light became important, the need to improve efficiency constituted a strong selection pressure for gene duplication. Gene duplication allowed the development of specialised Q_A and Q_B sites and the switching off of charge separation on the Q_B branch of the reaction centre.

Based on sequence comparisons, it seems that the L and M subunits of purple bacteria are more closely related to each other than the L is to the D1 subunit and than the M is to the D2 subunit [130]. The same applies to the relationship between the D1 and D2 subunits of PSII. This could be taken as indicating that the specialisation of the Q_A and Q_B quinone sites and the switching-off of charge separation on the Q_B side, have evolved twice. At the time, this was difficult to accept since it was the similarities between the quinones in particular that led to the homology modelling of PSII. While the interpretation of the sequence data has changed slightly and an escape clause has been offered from this conclusion, several factors conspire to make it more acceptable that Q_A/Q_B and the heterodimeric reaction centre could have evolved more than once. These factors include: i) the evident evolutionary pressures from the inefficiencies inherent in a homodimeric Type II reaction centre ancestor described above, ii) the very similar starting structures inherited from a common homodimeric ancestor and iii) the strong influence of the specific properties of quinone chemistry [23,88].

8. Q_A to Q_B electron transfer in purple bacteria as a basis for comparison with PSII

The electron transfer reactions associated with Q_A and Q_B in PSII are in many ways similar to those occurring in purple bacteria. Since the bacterial reaction centre is one of the best studied systems for proton-coupled electron transfer, a brief description of the bacterial reaction is useful as a basis for comparison with PSII.

The main features are as listed below, when differences exist in PSII, these will be noted. When these are significant, they will be discussed in subsequent sections. If no qualification is given, then the information is valid for PSII as well as purple bacterial reaction centres (or we forgot).

The two quinones are symmetrically located on either side of the non-heme iron, Fig. 6. Q_A is fixed and non-exchangeable in a relatively hydrophobic environment and is unable to undergo protonation. Q_B is exchangeable and is in a hydrophilic environment in contact with species that are able to deliver protons (ionisable amino acids and water). Q_A undergoes 1-electron redox reactions. It is reduced by the BPh^- forming the semiquinone anion, Q_A^-. Then electrons are transferred to Q_B in 100 μs [29] (400 μs in PSII) [80]. If Q_B^- is already present, Q_A^- transfers an electron more slowly, at about 1 ms [29] (0.6–0.8 ms in PSII) [80].

The Q_A^- to Q_B electron transfer is limited by a gating effect, which seems to involve movements of Q_B in its site, the formation of H-bonds, the protonation of protein groups close to Q_B^- and most likely conformational changes in the protein. This gating effect can not occur at low temperature and by freezing under illumination, the gate can be trapped in the open state [27,29,30].

The exact nature of the gating reaction is still under debate. Previously, the gating process was linked to a significant change in the position in Q_B from a distal to proximal position [131]. This is no longer held to be the gating reaction by most researchers in the field [132]. The so-called distal site is not now considered to be the stable binding location for Q_B under normal functional conditions, rather "a half way in" position that happens to be stable in some detergent solubilised proteins.

Several reactions occur that could contribute to the gating effect including the following. i) The formation of an additional hydrogen bond to the distal carbonyl of Q_B^- [133,134]. This occurs at physiological temperatures but cannot occur at 77 K [134]. ii) Evidence interpreted as arising from changes in the amino acids liganding the non-heme iron has recently been reported [135,136]. iii) Q_B^- formation is accompanied by the protonation of M-Glu212 close to the proximal carbonyl of the semiquinone. This protonation contributes to the stabilisation of the semiquinone [29,30].

The proton transfer pathway has been studied in some detail (reviewed in [29,30]). While less studied in PSII, Q_B^- is also stabilised by protonation although the groups involved and specific reactions occurring are not known (reviewed in [81]). Interestingly, FTIR studies indicate that the protonation reaction in PSII does not involve carboxylic acids [137]. In addition anomalous temperature dependence of electron transfer and of the structure around the non-heme iron have both been taken as evidence for a similar gating effect in PSII [138–140].

In purple bacterial reaction centres, the rate of the Q_A^- to Q_B^- step is limited by protonation reactions, (reviewed in [29,30]). When the $Q_A^-FeQ_B^-$ state is formed, the electrostatic effect of the charge on Q_A^- leads to protonation of Q_B^- at the distal carbonyl (the transient formation of the neutral $Q_BH^\bullet$ radical), before the electron is transferred. The monohydroquinone anion, Q_BH^-, is thought to be transiently formed before a second protonation takes place, presumably from the Glu212 to the carbonyl proximal to the iron. The protonation of the carbonyls and the absence of an electrostatic attraction allow the hydroquinone Q_BH_2, to be released from the quinone binding pocket. Presumably its hydrophobic tail is attracted back in to

lipid environment of the membrane. For PSII the current state of knowledge lacks these details; however something similar is likely occurring with some potentially significant differences that are discussed in more detail below.

The basic structural motif of this part of the purple reaction centres is common to PSII, Fig. 6. It is made up of two symmetrical quinones, each pinned in position by H-bonds to both carbonyls. The outer H-bonds come from backbone amides for both Q_A and Q_B, but for Q_B there appear to be additional H-bonds to the distal carbonyl [39], see Fig. 6. These additional H-bonds presumably contribute to stabilising the Q_B^- semiquinone relative to Q_A^- and thus contributing to the driving force required for forward electron transfer. The additional H-bonds may offer a way of regulating electron transfer, stabilising Q_B^- without allowing protonation. If Q_B^- were to undergo protonation, then it would likely lose one of its anchoring H-bonds and loosen the other. The consequent shift in its potential and its position, perhaps its loss from the site, would lead to inhibition of the second electron transfer step. The H-bonds to the proximal carbonyl group of the two quinones come from the histidines that ligand the non-heme iron. The "protein–Q–His–Fe–His–Q–protein" motif appears to be a good structure for electron transfer, with the two quinones held at a distance of 13 Å (edge to edge). At this distance electron transfer through protein could be faster than 0.4 μs, the theoretical rate maximum based on the distance [141]. The actual rates are much slower than this (400 μs–1 ms) presumably due to movements of the quinone, the protein and protons.

The role of the iron remains somewhat enigmatic. A series of observations is usually rolled out at this point to illustrate the unimportance of the iron to electron transfer. The most telling of which is probably the replacement of the iron with Zn^{2+}, a non-redox metal, resulting in no change to the kinetics of electron transfer [142]. Clearly the iron plays an important structural role, not only as the central component in the Q–His–Fe–His–Q motif but also in holding the two halves of the reaction centre together. It seems likely that this structural integrity is important for transferring information between the two quinone sites and the various protonable groups (see [136]). The overall positive charges on the metal also is predicted to have an important electrostatic effect as well as strengthening the H-bonds from the liganding imidazoles to the quinones and these are expected to increase the redox potentials of the quinone redox couples [143]. The non-heme iron in PSII clearly plays a similar role (see [144] for a recent discussion), however its chemistry is more complex and thus may have more mechanistic roles. These will be described below.

Overall then, many of the characteristics of the Q_AFeQ_B complex of purple bacteria are also present in PSII. There are however several properties of the quinone complex of PSII that differ from those seen in the purple bacterial reaction centre. These presumably reflect functional differences. These differences will be dealt with specifically in the next section.

9. The quinone–iron complex in PSII and purple bacterial reaction centres: the same… but different

9.1. Q_A redox switching

The redox potential of Q_A is high (65 mV) when PSII lacks the donor-side Ca^{2+} ion [145,146]. Since the Mn provides the binding site for the Ca^{2+}, then the high potential form is present in PSII before the Mn_4Ca cluster is assembled [72]. Upon cluster assembly, the redox potential switches to a form that is around 150 mV lower in potential (−80 mV) [72,146]. The magnitude of the redox potential shift was recently verified although the absolute values for the Q_A redox couples were both found to be 60 mV lower [147] (see however [148]). This redox switching is rationalised in terms of a mechanism for protecting PSII from photodamage under conditions where the electron donation from water cannot occur. Two kinds of photodamage are expected under such conditions.

The first kind of photodamage is expected to arise from over-oxidation reactions that occur due to abnormally long life-times of oxidising species such as P^+ and $TyrZ^+$ in the absence of a functional electron donor system. It is known that a side-path of electron donation will provide electrons to P^+ under these conditions (see Fig. 4) [68,69]. However, electron donation from this pathway is slow, in the millisecond timescale; and millisecond lifetimes for P^+ could lead to oxidative damage. In addition, over-oxidation of the side-path donors themselves (β-carotene and $ChlZ_{D2}$) could also be a problem [68], especially since it is thought that they can be reduced under some conditions by other chlorophylls and carotenoids in and around the reaction centre [149]. Over-oxidised organic species can lead to a range of uncontrolled reactions with protein residues or other pigments. Oxidative damage to the carotenoids themselves and modifications of the chlorophyll-bearing proteins could lead to chlorophylls becoming uncoupled from their protective carotenoids and thus allowing them to be the source of triplet-mediated $^1O_2$ formation, which could initiate a chain reaction of photodamage.

The second type of photodamage predicted in PSII with a non-functional donor side results from the back-reaction of the $P_{D1}^+Q_A^-$ to the $P_{D1}^+Ph_{D1}^-$ state which can recombine to generate the reaction centre chlorophyll triplet state [102,146,150]. This triplet state can react with $^3O_2$ to produce singlet oxygen ($^1O_2$) which is responsible for photodamage [150,151]. The central pigments (i.e. Chl_{D1}, on which the triplet is formed [22,49], P_{D1}, P_{D2}, Chl_{D2} and the two pheophytins) are all too far from the nearest carotenoid to be efficiently quenched; the Ch_{D1} to Car_{D1} distance is 20 Å; and that for Chl_{D2} to Car_{D2} is 13 Å (see Fig. 4) [39]. By having a high potential Q_A both of these kinds of photodamage can be limited or eliminated.

The over-oxidation damage will be mitigated by less efficient electron transfer out of the reaction centres. The drop off in the driving force between Q_A and Q_B means that the $Q_A^-Q_B \leftrightarrow Q_AQ_B^-$ and the $Q_A^-Q_B^- \leftrightarrow Q_AQ_BH_2$ equilibria would be shifted to the left. It is quite possible that the redox properties of Q_B are also changed by the absence of Ca^{2+} (or the entire Mn_4Ca cluster). However the overall driving force for the electron donation from Q_A^- to the quinone pool will certainly be 150 mV less than in the active system. Since Q_A reduction is not associated with a protonation [81] while Q_B and plastoquinone reduction are both proton-coupled, then the driving force for electron transfer is expected to decrease at higher pH values. It seems likely then that under physiological conditions (with the acceptor side is exposed to pH>7.5), forward electron transfer will be inhibited to some extent when Q_A is in its high potential form, leading to less over-oxidation on the donor side [72].

When dealing with over-oxidation, it would be beneficial if the side pathway, or rather the complete cyclic version of it, were more functional prior to Mn_4Ca cluster assembly or when Ca^{2+} is absent. As far as we are aware, however, this has not been seen (yet). Intriguingly, changes in Cyt *b*559 function have been reported during photoactivation [152] and changes in the redox potential can be affected by the presence of Ca^{2+} in the absence of some of the extrinsic polypeptides [153].

The back-reaction mediated photodamage will be mitigated by a change in the back-reaction pathway. The shift to the high potential form of the Q_A means that the energy gap between $P_{D1}^+Q_A^-$ and $P_{D1}^+Ph_{D1}^-$ pair is so great that back reaction is greatly disfavoured. In this way $P_{D1}^+Ph_{D1}^-$ recombination, reaction centre triplet formation and hence singlet O_2 formation are minimised [72].

There is no evidence for this kind of redox switching in purple bacteria. It is simply not necessary. The chemistry is not as oxidising and the radical pair recombination triplet, should it occur, is quenched by a carotenoid that is in van der Waals contact with $BChl_M$, (unlike the situation in PSII, the carotenoid in purple bacterial reaction centres can be close to P^+ without being oxidised). However, these

two different types of back-reaction pathway described in PSII do exist in purple bacterial species. In *Rhodobacter spheroides* the energy gap is big, like that in PSII in the absence of the Mn_4Ca cluster, with charge recombination occurring slowly by a direct route [154,155]. In *Rhodopseudomonas viridis*, the energy gap is smaller, like that in functional PSII, and the back-reaction takes place with the formation of the $P^+BPh_L^-$ radical pair and thence the ^3P triplet [156]. The small energy gap in *R. viridis* may simply be due to the smaller driving force inherent in using bacteriochlorophyll *b* with P at 960 nm. This squeezes the energy gaps between P* and the quinone pool and the smaller energy gap between $P^+BPh_L^-$ and $P^+Q_A^-$ may be inevitable. *R. viridis* is a microaerophilic organism and so it does not have to deal with photodamage from triplet-mediated $^1O_2$ formation.

The structural origin of the Q_A redox switching in PSII is not known. Correlating other differences occurring under similar conditions, it is worth considering that the redox change may be related to the two structural forms manifest as the EPR signals at g = 1.9 (intact functional PSII, in the presence of (bi)carbonate) and g = 1.82 (damaged PSII or in the presence of formate, see below). In Mn-depleted PSII from plants, the g = 1.82 form was present below pH 7.5, while the g = 1.9 form was present above that pH [111]. Under similar conditions H-bonding-mediated coupling between the nitrogen nucleus of D2-His214 (Fig. 6) and the electron spin on the Q_A^- was also lost at pH values above pH 7.5 [62]. This change in magnetic coupling could be due to the ionisation of a group close to the Fe, possibly with the bicarbonate deprotonating to form carbonate (see [114]).

An alternative explanation arose from analysis of the crystal structure. Ishikita and Knapp [157] found two possible positions for D2-Thr217: one with the –OH group H-bonded to the Q_A carbonyl proximal to the iron and the other with the –OH rotated so that the proton turned away from the quinone and H-bonded the nearby D2-Trp253. Their electrostatic calculations indicated that the presence of the H-bond to Q_A would result in a 150 mV difference in the E_m of Q_A: the same difference as seen experimentally. This seemed to be more than a coincidence. It is also possible that the presence and absence of the additional H-bond to the proximal carbonyl of the Q_A^- could be responsible for the change in magnetic coupling of the electron spin to the nuclear spin on the H-bonded histidine reported in [63].

The influence of the Ca^{2+} of the Mn_4Ca cluster [145,146], on the electron acceptor side was quite difficult to accept. The Mn_4Ca site is located in the D1 subunit, 38 Å away from the Q_A site in the D2 subunit. On the other hand, the D1 and D2 polypetides are each made up 5 transmembrane helices that are wrapped around each other to some extent and the isoprenyl tail of Q_A penetrates well down into the reaction centre and gets very close to Chl_{D1} [39,40]. The redox propeties of Q_A itself are sensitive to changes in the Fe environment (provided by both D1 and D2) and to occupation of the Q_B site (in D1) [158]. Furthermore, assembly of the Mn_4Ca cluster, including Ca^{2+} binding, is thought to involve conformational changes [159–161] and it is thought that the conformational change may be specifically associated with Ca^{2+} binding. Such a conformational change may be relayed to the acceptor side. A crystal structure of the Mn_4Ca-depleted enzyme would be of interest here.

It has been known for some years that the binding properties of the Ca^{2+} vary depending on the intermediate states (S states) of the charge accumulating enzyme [162]. In PSII lacking the 23 kDa extrinsic polypeptides, the Ca^{2+} is easily exchangeable in the S_3 state but sequestered in S_1 and S_2 states. This is assumed to reflect structural changes, a weaker binding site for Ca^{2+}, perhaps one less ligand to the Ca^{2+} in the S_3 state and this is reflected in conformation changes detectable by X-ray absorption [163]. Given that binding and de-binding of the Ca^{2+} influences the potential of Q_A during photoactivation [72], then it is worth considering the possibility that something similar may occur in the different steps of the S state cycle. This could allow some kind of tuning of the forward and back-reaction rates to suit the lifetime of the given S state: for example Q_A^- could be stabilised or transferred more rapidly to Q_B in the last steps of the cycle where electron donation steps from the TyrZ and the Mn_4Ca/water system are slower. There are however conflicting reports on the S-state dependence of Q_A^- oxidation (see for example [80] and [164]) but this is worth readdressing, looking for Ca^{2+}-associated changes in S_3.

It is also worth noting that the effect on Q_A from the donor side is known because Q_A is an easy component to measure. The redox properties of the iron and Q_B are less commonly measured and it is also possible that they too are influenced by changes occurring on the electron donor side, especially since they both share the same protein subunit (D1) as the Mn_4Ca cluster. It would be interesting to look for redox shifts induced from the donor side.

9.2. In PSII there is more protein between Q_B and the membrane

While the central pair of subunits and their cofactors are similar in purple bacterial reaction centres (L and M) and PSII (D1 and D2), the other subunits are quite different. Purple bacteria have a large globular protein, the H subunit, that caps the electron acceptor side. In the membrane the bacterial reaction centre is surrounded by a ring of antenna proteins but these are not tightly bound. It is thought that the quinone has access directly from the membrane to the quinone site via a short shallow channel the length of only 1 isoprenoid group. The tail of the quinone remains in contact with the lipid.

In PSII there appears to be no H subunit and no other capping proteins are present in the crystal structure [55,56]. The Q_B side of the D1D2 pair is flanked by Cyt *b*559 and two small subunits Y and J [40,55–57,129]. Thus the Q_B site is relatively distant from the membrane and the quinone pool. Access is made possible through a channel that is as long as the entire isoprenoid chain [40].

9.3. Q_B, Q_C and their channels

The crystal structure shows a rather complex arrangement of channels and cavities in PSII associated with Q_B. Of special note is the presence of a third quinone designated Q_C in [40] not observed in [39]. Evidence for a third quinone in isolated PSII cores from *Thermosynechococcus elongatus* was reported from functional studies showing two cycles of Q_B^- formation on a flash sequence [140] and from quinone quantitation studies of the preparations used for crystallography [165]. Mechanistic studies using the inhibitor, DCMU, had already led to the suggestion of a second exchangeable quinone binding site in the environment of Cyt *b*559 [166,167] in plant PSII. Whether all of these effects reflect the same site is unclear. Indeed the Q_C site in the crystal structure is completely different from the Q_A and Q_B sites, having no contacts to the head group from the protein and instead only having contact to a lipid patch on the interior surface of the channel. It is unlikely that the semiquinone would be stabilised in this site. This also probably means that this does not correspond to the DCMU binding site in the earlier studies [166] and thus another binding site may exist in the region of the Cyt *b*559.

In the crystal structure, the tail of Q_B is threaded down one channel while that from Q_C goes down another [40]. Various interpretations were given, one of which is that the channels represent an "out" channel by which Q_B leaves and an "in" channel by which Q_C loads. The reported Q_C site of the crystal structure could exist in order to diminish the change-over time for replacing Q_BH_2 with a quinone from the pool (see [40] for detailed discussion). The exchange time might be expected to be much longer in PSII with its long tortuous channels compared to the situation in purple bacteria. Having a preloaded quinone close to the Q_B site may be a good solution to this problem. Indeed de Wijn and van Gorkom [80] found two slow phases of Q_A^- oxidation that they attributed to forward electron transfer to Q_B, i) when Q_A^- is formed in the presence of an empty Q_B ($t_{1/2}$ = 2–3 ms) and ii) when Q_A^- is formed in the presence of Q_BH_2 ($t_{1/2}$ = 100 ms). It

is possible that these values could instead represent quinone entering the site from the near-by Q_C site vs. quinone entering from the pool.

9.4. Protective (futile) cycles: reduction of Cyt b559 by reduced quinone

The two quinone channels pass on either side of the Cyt *b*559 heme and the nearest part of Q_B and Q_C tails to the heme edge is 11 Å and 6 Å respectively. This means that the reduced hydroquinone head must pass within this distance of the heme on its way out. When the Cyt *b*559 is oxidised and in its high potential form (390 mV), there may be sufficient driving force for the reduction of the heme by one electron from the QH_2, forming the unstable semiquinone. The unstable Q^- would be quite capable of reducing O_2 if it encountered it. There are several reports implicating Cyt *b*559 in O_2 redox chemistry [167–169] and a semiquinone mediated mechanism could be involved. Alternatively, the semiquinone might prefer the stability of the Q_B site and 1-electron reduction of the Cyt *b*559 by QH_2 could lead to formation of Q_B^-.

The 25 Å distance between the Q_B site and Cyt *b*559 will allow in the electron transfer in the millisecond timescale, as discussed in Petrouleas and Crofts [81]. This may be too slow for a protective cycle. The donation from somewhere down the Q_B channel (perhaps one of the "Q_C sites" mentioned above [40,166,167]), would give rates that could be of more functional relevance in a protective cycle.

In the protective cycle, it is thought that electrons arrive at P_{D1}^+ in a few milliseconds from the β-carotene, Car_{D2} (Fig. 4), as the initial donor [170], perhaps with Chl_{D2} as redox intermediate [68]. The Car_{D2} cation radical is a branch point, with electrons coming from the Cyt *b*559 or from the $ChlZ_{D2}$ [170]. Because of its lower potential, the reduced Cyt *b*559 is the dominant donor with neither Car_{D2} nor $ChlZ_{D2}$ cations being detectable. The reduction of the heme by quinol completes the cycle at room temperature [171]. Cyt *b*559 reduction at room temperature has been observed and is sensitive to DCMU, an inhibitor that binds in the Q_B site [171]. It has been suggested that this side-path or cyclic electron transfer chain may exist in order to provide electrons to P_{D1}^+ under conditions where other electrons (from TyrZ, the Mn and water, from back reactions, or from TyrD) are not forthcoming and thus it would provide some kind of protection against over oxidation [172] reviewed in (see section 9.1 above). Given the slowness of the donation under optimal conditions, an alternative explanation of this pathway was suggested [68]: that the side-path cycle was there in order to reduce the Car_{D2} cation radical, which is inevitably formed with a low quantum yield because of the proximity of this pigment to the most oxidising species in the reaction centre. In this "save-the-carotene" model, the position of the Car_{D2} is considered to be at a compromise position: just far enough away from the core of the reaction centre to minimise its electron transfer rate but close enough to play a role in quenching, chlorophyll triplet and O_2 singlet.

In the next section (and earlier in this article), we reconsider the rate question in the futile cycle and suggest that it could work to protect against over-oxidation damage provided the its electron donation rate to P^+ rate is drastically increased under specific conditions.

9.5. Efficient switching on and off of a protective cycle in some species

PSII from marine plankton, which are exposed to big variations in light, show a very marked protective mechanism that appears to be a switch from linear electron flow to a protective cycle around PSII [173,174]. This is linked to the reduction state of the plastoquinone pool presumably by some kind of switch. The most likely pathway for cyclic electron transfer is the QH_2-Cyt *b*559-Car_{D2}-P_{D1} pathway described above, see Fig. 4. An acceptor side switch, should it exist, could for example be triggered by the formation of Q_A^- before the Q_BH_2 has left the site or formation of Q_B^- before QH_2 has cleared the channel and remains in the vicinity of the heme. Electron donation from QH_2 from a possible site in one of the channels to oxidised (high potential) Cyt *b*559, may occur as discussed above. The well-known but poorly understood high/intermediate/low potential forms of the Cyt *b*559 may relate to this switch [175].

For this to work, Cyt *b*559 must already be oxidised and for this to occur as part of an efficient protective cycle, the side-path must be able to donate more rapidly to P_{D1}^+. As mentioned above, in plant and cyanobacterial PSII, the side-pathway seems to work rather inefficiently, with donation times from Car_{D2} to P_{D1}^+ estimated to be in the millisecond timescale at room temperature [68,176]. Donation from TyrZ occurs in tens-hundreds of nanoseconds, and the $P_{D1}^+Q_A^-$ back reaction takes place in 200 μs in plant PSII and 1 ms in cyanobacteria [193]. We might speculate that to work efficiently, the side pathway needs to be "switched on". One way for this to occur would be for the chlorophyll cation to change its localisation from P_{D1} (which is 21 Å from Car_{D2}, see Fig. 4) by electron transfer over towards Chl_{D2}, (which is 9 Å from Car_{D2}) through a change in the relative potentials of the chlorophylls. Even a small shift in the equilibrium towards Chl_{D2} would drastically speed up oxidation of the β-carotene [141].

One can speculate about switching mechanisms, perhaps involving electrostatic or structural effects from the donor or acceptor sides (see below) but before getting carried away, the role of the known side-path components in the protective electron transfer cycle should be tested directly in the marine plankton. Indeed, with the current limited knowledge, several alternative routes cannot be ruled out. For example, a route involving a carotenoid found in the interface of the D1 protein and the T subunit, named Car104 in [177], is located at only 16 Å from Q_A. A Q_A-Car104-$ChlZ_{D1}$-P_{D1} cycle has been suggested (Fig. 4), based on this short distance and the presence of Car104 in a cluster of 4 other carotenes that approaches $ChlZ_{D1}$ [177]. $ChlZ_{D1}$ however will always be a slow donor to P_{D1}^+ given its location 21 Å from Chl_{D1}, the closest of the central pigments. A second alternative may involve the Cyt *c*550, which has recently been shown to have a potential high enough for it to exist in a reduced state under physiological conditions [178]. It is thus available for donating electrons to the long-lived S states. Again donation will be slow since its distance from the Mn_4Ca cluster in the cyanobacteria is at least 23 Å. It will be interesting to see if this distance is shorter in the phytoplankton. Re-reduction of Cyt *c*550, should it occur, would likely be from a soluble electron-donor in the lumen.

Whatever the mechanism, the switching on and off of this protective cycle is remarkable. When the plastoquinone pool is reduced there is a major photochemical "miss". Its mechanism is worthy of further investigation since it is likely that it works in PSII of other species, albeit to a less dramatic extent. It is also worth noting that some sort of switch process occurs on the first couple of turnovers during photoactivation; in addition, the photoassembly of the Mn_4Ca cluster appears to involve a change in the redox state and form of Cyt *b*559 [152]. It would make sense that some kind of change from a protective, cyclic flow to functional linear electron flow may occur during certain steps of photoassembly of the Mn_4Ca.

9.6. No H subunit in PSII: access to the Fe^{2+}?

The H subunit is the third subunit of the bacterial reaction centre. It is a mainly globular protein that caps the acceptor side of the protein. It contains channels that allow proton access to the Q_B site. The channel entrance binds a Zn^{2+} ion and the channel can be blocked to some extent by binding of other metals (reviewed in [30]). This subunit is absent in PSII. In cyanobacteria, PSII binds the very large phycobilisomes on the stromal surface of the membrane and these may restrict some access, but since the contact for energy transfer must be to the antenna chlorophylls that are peripheral to the complex [179] there might be still enough open space for access to the non-heme iron. In plant PSII at least and possibly in cyanobacterial PSII, the region around the quinone–iron complex seems to be much more exposed to the aqueous medium than in the bacterial reaction

centre (Fig. 7). The distance from the Fe to the aqueous phase is estimated to be 20 Å in the purple bacterial reaction centre and 10 Å in PSII. In PSII this corresponds to the bicarbonate/carbonate ligand H-bonded via 2 water molecules to a glutamate, which is exposed to the aqueous medium (see Figs. 6 and 7). This difference is probably relevant to quinone related proton-coupled electron transfer (see [137]).

9.7. The oxidisable non-heme iron in PSII

The non-heme iron in PSII is oxidisable under mild conditions with a pH dependent E_m of 400 mV at pH 7. Once oxidised, it can be reduced rapidly ($t_{1/2} = 25$ μs) [180] by electron donation from Q_A^-. The potential of the Fe^{2+} is modulated by the nature of the exchangeable ligand and the occupancy of the Q_B site by herbicides [181]. The Fe^{2+} is oxidisable by some artificial quinones added as electron acceptors to PSII, such as phenyl-*p*-benzoquinone, PPBQ [182]. The first electron to arrive at the artificial quinone reduces it to its semiquinone form. The semiquinone is oxidising enough to remove an electron from the nearby iron forming the Fe^{3+} state. On the subsequent flash, the Q_A^- then donates rapidly producing the Fe^{2+} state [182]. When such an artificial quinone is present, a series of saturating flashes gives rise to a period-of-two oscillation in the redox state of the iron, being oxidised on the first flash and odd-numbered flashes and reduced on the second and even-numbered flashes.

The possibility that this mode of electron transfer out of the reaction centre might occur in native PSII has been considered. The oxidation of Fe^{2+} in a fraction of centres has been observed in dark-adapted PSII samples. Reports have appeared of some Fe^{2+} oxidation without the addition of a specific chemical oxidant. Nugent [183] reported Fe^{2+} oxidation when semiquinone and oxygen were present. The mechanism of this reaction was not clear. Boussac and co-workers [184] reported Fe^{2+} oxidation when DCMU was added to a sample containing Q_B^-, and this was explained by the following reaction:

$$Fe^{2+}Q_B^- + DCMU \leftrightarrow Fe^{3+}Q_BH_2 + DCMU \leftrightarrow Fe^{3+}DCMU + Q_BH_2$$

with the strong binding of the herbicide pulling the equilibrium to the right, favouring formation of the oxidised iron. Recently, it was observed that when Q_B^- is formed, Fe^{3+} is formed slowly in the dark in a fraction of centres even in the absence of O_2 [185]. This reaction is simply $Fe^{2+}Q_B^- \rightarrow Fe^{3+} + Q_BH_2$. This occurs slowly and in only a fraction of the centres (about 10%) but it does show that this reaction can occur in untreated PSII. It is thus possible that under certain conditions it may occur more rapidly and/or in a greater fraction of the centres. This mode of electron transfer is one that would be predicted to be beneficial. It eliminates the long-lived Q_B^- state in the reaction centre, this prevents charge recombination with S_2 and S_3 states. This means that these S states will be longer lived (see [81,83,84]) and chlorophyll triplet mediated photodamage will not occur [150]. Thus the Fe^{2+} oxidation mode of quinol formation would be particularly advantageous in low light.

With such advantages, the question arises: why has this mode of electron transfer not been selected by evolution? There must be a problem. The answer is probably the rate. We assume that the reaction is the following,

$$Fe^{2+}Q_B^- \leftrightarrow Fe^{3+}Q_BH_2 \leftrightarrow Fe^{3+} + PQH_2$$

where the first equilibrium is far to the left, and the second is to the right. Nugent [183] ruled this reaction out because the Q_B^-/Q_BH_2 couple is much too low (perhaps 90 mV assuming a similar semiquinone stability as in purple bacteria) to be able to oxidise the Fe^{2+} (E_m 430 mV at pH 6.5). However, if we take into account the release of the Q_BH_2, then the energy associated with stabilising the semiquinone is regained and thus iron oxidation becomes favourable. The stabilisation of Q_B^- has meant that iron oxidation will be disfavoured and slow; this may be the reason why PSII does not take advantage of this mode of quinone reduction.

Another factor that could have an important role in iron oxidation is the charge on the carboxylic acid will likely affect the potential of the Fe^{2+}/Fe^{3+}, with more negative potentials with CO_3^{2-} (carbonate) compared to HCO_3^- (bicarbonate). The bicarbonate-iron vs. carbonate-iron could represent switchable high and low potential forms.

The Fe^{2+} in purple bacterial reaction centres does not undergo oxidation with oxidants or with artificial quinones [186,187]. This presumably reflects the iron environment. Relevant in this regard, the Fe^{2+} in PSII is less sequestered, has more flexibility in its ligands and has a carboxylate ligand that can undergo a deprotonation (bicarbonate to carbonate), which would stabilise the Fe^{3+} state.

In considering the evolution of the Type II reaction centres, it has been suggested ([13,23] and see section 7) that an ancestral homodimer would perform quinone reduction through the dismutation of two identical semiquinones. In the light of the new observations of iron oxidation by Q_B^- described above, it worth considering the alternative possibility that quinone reduction may have occurred in the homodimer through an iron oxidation mechanism (unstable Q^- oxidising Fe^{2+} forming QH_2 and Fe^{3+}, followed by Q^- reduction

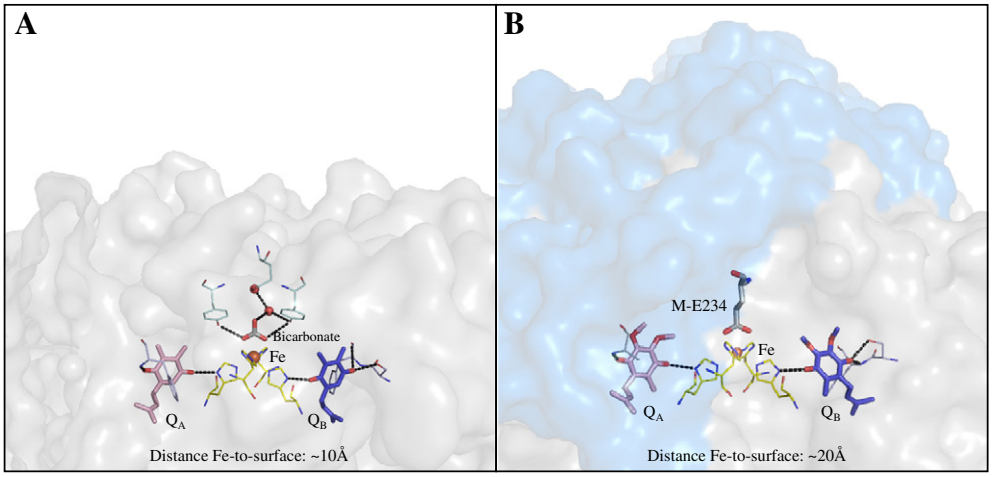

Fig. 7. A perspective view of the Q_AFeQ_B electron acceptor complex in (A) PSII and the purple bacterial reaction centre depicting the exterior surface of the reaction centre proteins. In panel (B) the blue surface belongs to the H subunit that caps the reaction centre of purple bacteria.

of Fe^{3+} on the second turnover). In principle, with a poorly stabilised semiquinone, this mechanism would work more rapidly and would overcome at least one of the inefficiencies listed in section 7 (while most likely presenting new ones). The presence of slow iron oxidation by Q_B^- in PSII may represent an evolutionary remnant of the old homodimer days.

9.8. Exchangeable ligand: bicarbonate and formate effects

While the ligand environment around the non-heme iron is ostensibly similar in PSII and purple bacterial reaction centres, there is one major difference. The carboxylic acid that provides a bidentate ligand in addition to the four histidine imidazoles, is a glutamate (M-E232, as shown in Fig. 6) in purple bacteria but a bicarbonate in PSII [10,112,113]. Bicarbonate is an exchangeable ligand. Exchanging it for other carboxylic acids inhibits electron transfer. With formate instead of bicarbonate, electron transfer from Q_A^- to Q_B is slowed by a factor of 5, from Q_A^- to Q_B^- is slowed by a factor of 10 and the exchange of Q_BH_2 with the pool is slowed also by more than a factor of 10 [188–190] and given that this is the rate-limiting step, this has a major effect on function.

It is not clear why formate and the other carboxylic acids should have these inhibitory effects. It has been suggested that the bicarbonate may play a role in protonation during the reduction of Q_B [191]. This seems very reasonable but there is little experimental evidence for this. The special feature of bicarbonate compared to formate and other small carboxylic acids is that it can undergo a further ionisation and become a carbonate dianion. It has been suggested that carbonate may be the ligand to the iron in intact PSII. This suggestion arose from simulations of the EPR spectra and from molecular calculations [114]. In contrast, FTIR studies indicated that bicarbonate rather than carbonate was present [113]. However the Mn-depleted plant PSII preparations, which were used for the FTIR experiment, would be predicted to show the non-native form of the $Q_A^-Fe^{2+}$ state, as seen by EPR, and thus it would correspond to bicarbonate rather than carbonate under these conditions. To test this, the FTIR experiment needs to be done on the intact PSII.

The EPR signals from $Q_A^-Fe^{2+}$ in native PSII are not similar to those seen in purple bacteria. The PSII signals are weak and show a broad feature at $g = 1.9$ rather than the well-known bacterial signal at $g = 1.84$ [111]. Addition of formate (and other carboxylic acids) results in the conversion of the PSII-type signal into a strong $g = 1.84$ signal typical of purple bacteria. This also occurs for $Q_B^-Fe^{2+}$ [192]. In formate-treated PSII, the $Q_A^-Fe^{2+}$ signal is modified upon the reduction of the secondary quinones by two electrons. Thus $Q_A^-Fe^{2+}$ seems to be sensitive to the occupation of the Q_B site by Q_BH_2. It seems that the formate-inhibited state is one in which Q_BH_2 remains in its site, rather than slow loading of plastoquinone back into the site [192]. Despite these new observations, the inhibitory effects of formate remain poorly understood at a chemical level and require further study.

The question arises whether carboxylic acid binding to the iron could have any relevance to the regulation of electron transfer out of PSII. This has been discussed before and it was considered that natural concentrations of glycolate, a carboxylate ion that down-shifts the potential of the iron thus making it more easily oxidisable by the semiquinone, were too low to be mechanistically important [181]. Perhaps just the change from bicarbonate to carbonate, through tuning of the pKa of the carboxylic acid could be mechanistically relevant. Clearly the presence and absence of the additional charge is liable to have significant mechanistic effects. Once again it is worth considering such tuning effect could come from the electron donor side and whether the changes in the ionisation state of the carboxylic acid could be sensed by the electron donor side. Major switching processes likely occur during assembly (and disassembly) of the Mn_4Ca cluster, so investigations of the role and nature of the carboxylic acid during these processes will perhaps be worthwhile.

9.9. Structural aspects not directly associated to electron and proton transfer

As bioenergeticists, we have a tendency to look for explanations in terms of electron transfer and proton transfer reactions. Sometimes it is worth remembering that other processes do exist in biology. PSII is very different from the purple bacterial reaction centre in that it is damaged and disabled about every 30 min under normal functional conditions. It seems that the damaged PSII complex, a dimeric system (at least in cyanobacteria), in which each monomeric unit is made of more than 20 polypetides, is disassembled in order to remove the damaged D1 protein and replace it with a freshly made copy. The D1 protein provides the main protein ligands and environment for half of the reaction centre pigments, for the Mn_4Ca cluster (except for the ligand Glu354 from the CP43 antenna protein [57]), and two of the four histidine residues to the non-heme iron that holds the reaction centre together. What happens during the removal and replacement of the D1 subunit? We do not yet know but it is not impossible to imagine that some of the differences in the structural properties of the non-heme iron compared to the bacterial reaction centre reflect the need to disassemble and reassemble the complex rapidly and repeatedly. Taking this idea to its extreme, one might postulate that the oxidisable iron and the exchangeable bicarbonate ligand could be a simply side-effects of these structural requirements.

10. Conclusion

PSII and purple bacterial reaction centres have fundamental similarities, however detailed comparisons show many differences. The recent crystal structures have provided a more solid basis for the understanding of these differences. Many of the factors that have allowed PSII to attain very high oxidising powers have been elucidated based on chemical insights, the crystal structure and theoretical calculations. These give new perspectives on how these functions could have evolved. Many differences between PSII and purple bacteria are best explained in terms of protection mechanisms that are required because of the highly oxidising chemistry associated with water oxidation in PSII. Despite these protection mechanisms, the enzyme is photodamaged and repaired relatively rapidly and often. Some putative protection mechanisms can most easily be rationalised assuming a role during the repair and assembly processes themselves. Real demonstrations of these protective mechanisms in action are lacking. Future research needs to focus on the study of intermediates in the repair and assembly cycle, looking for evidence of specific protective mechanisms and establishing when switches occur from one mode of function to another. PSII, the most complicated of reaction centres, continues to surprise us with new and unexplained features. These are worth exploring not only because the photodamage of PSII is often (i.e., under stress conditions) the process that limits the growth of the photosynthetic organism (and hence crop yields, biofuel yields, or survival) but also because it is simply a unique and fascinating enzyme.

Acknowledgements

This work was supported by the EU/Energy Network project SOLAR-H2 (FP7 contract 212508), T.C. is supported by the CEA Eurotalents programme, A. S. is supported by the IRTELIS training programme of the CEA and AWR is a recipient of the Wolfson Merit Award of the Royal Society. We would like to thank Alain Boussac, Wolfgang Nitschke, Anja Krieger-Lizskay, Klaus Brettel, Alberto Mezzetti and Fabrice Rapapport for helpful discussion.

References

[1] G.S. Beddard, G. Porter, G.M. Weese, Model systems for photosynthesis. V. Electron transfer between chlorophyll and quinones in a lecithin matrix, Proc R Soc London A 342 (1975) 317–325.
[2] R.E. Blankenship, Molecular mechanisms of Photosynthesis, Blackwell science Ltd., Oxford/Malden, 2002.
[3] N. Nelson, C.F. Yocum, Structure and function of Photosystems I and II, Annu Rev Plant Biol 57 (2006) 521–565.
[4] B. Schoepp, P. Parot, L. Menin, J. Gaillard, P. Richaud, A. Vermeglio, *In vivo* participation of a high-potential iron–sulfur protein as electron-donor to the photochemical reaction center of *Rubrivivax gelatinosus*, Biochemistry 34 (1995) 11736–11742.
[5] A. Hochkoeppler, S. Ciurli, G. Venturoli, D. Zannoni, The high-potential iron–sulfur protein (HiPIP) from *Rhodoferax fermentans* is competent in photosynthetic electron-transfer, FEBS Lett 357 (1995) 70–74.
[6] T. Wydrzynski, S. Satoh, Photosystem II: the light-driven water:plastoquinone oxidoreductase, Springer, Dordrecht, 2005.
[7] H. Dau, M. Haumann, The manganese complex of Photosystem II in its reaction cycle — basic framework and possible realization at the atomic level, Coord Chem Rev 252 (2008) 273–295.
[8] D.J. Des Marais, Evolution — when did photosynthesis emerge on earth? Science 289 (2000) 1703–1705.
[9] T. Cavalier-Smith, Cell evolution and Earth history: stasis and revolution, Philos Trans R Soc B 361 (2006) 969–1006.
[10] H. Michel, J. Deisenhofer, Relevance of the photosynthetic reaction center from purple bacteria to the structure of Photosystem II, Biochemistry 27 (1988) 1–7.
[11] A.W. Rutherford, Photosystem II, the water-splitting enzyme, Trends Biochem Sci 14 (1989) 227–232.
[12] L. Kalman, J.C. Williams, J.P. Allen, Comparison of bacterial reaction centers and Photosystem II, Photosynth Res 98 (2008) 643–655.
[13] A.W. Rutherford, P. Faller, The heart of photosynthesis in glorious 3D, Trends Biochem Sci 26 (2001) 341–344.
[14] N.W. Woodbury, J.P. Allen, The pathway, kinetics and thermodynamics of electron transfer in wild type and mutant reaction centers of purple nonsulfur bacteria, in: R.E. Blankenship, M.T. Madigan, C.E. Bauer (Eds.), Anoxygenic photosynthetic bacteria: advances in photosynthesis, Kluwer Academic Publishers, Dordrecht, 1995, pp. 527–557.
[15] A.J. Hoff, J. Amesz, Visible absorption spectroscopy of chlorophylls, in: H. Scheer (Ed.), chlorophylls, CRC Press Inc., Boca Raton, FL, 1991, pp. 723–738.
[16] T. Renger, E. Schlodder, Primary photophysical processes in Photosystem II: bridging the gap between crystal structure and optical spectra, Chemphyschem 11 (2010) 1141–1153.
[17] K.J. Kaufmann, P.L. Dutton, T.L. Netzel, J.S. Leigh, P.M. Rentzepis, Picosecond kinetics of events leading to reaction center bacteriochlorophyll oxidation, Science 188 (1975) 1301–1304.
[18] M.G. Rockley, M.W. Windsor, R.J. Cogdell, W.W. Parson, picosecond detection of an intermediate in photochemical reaction of bacterial photosynthesis, Proc Natl Acad Sci U S A 72 (1975) 2251–2255.
[19] W. Holzapfel, U. Finkele, W. Kaiser, D. Oesterhelt, H. Scheer, H.U. Stilz, W. Zinth, Observation of a bacteriochlorophyll anion radical during the primary charge separation in a reaction center, Chem Phys Lett 160 (1989) 1–7.
[20] M.E. van Brederode, R. van Grondelle, New and unexpected routes for ultrafast electron transfer in photosynthetic reaction centers, FEBS Lett 455 (1999) 1–7.
[21] A.W. Rutherford, Photosystem II, the oxygen evolving photosystem, in: S. Stevens, D.A. Bryant (Eds.), Light-energy transduction in photosynthesis: higher plant and bacterial models, American Society of Plant Physiology, Rockville, 1988, pp. 163–177.
[22] F.J.E. van Mieghem, K. Satoh, A.W. Rutherford, A chlorophyll tilted 30° relative to the membrane in the Photosystem II reaction center, Biochim Biophys Acta 1058 (1991) 379–385.
[23] A.W. Rutherford, W. Nitschke, Photosystem II and the quinone–iron-containing reaction centers: comparisons and evolutionary perspectives, in: H. Baltscheffsky (Ed.), Origin and evolution of biological energy conversion, CVH, New York, 1996, pp. 143–175.
[24] K.J. Kaufmann, K.M. Petty, P.L. Dutton, P.M. Rentzepis, Picosecond kinetics in reaction centers of *Rps sphaeroides* and effects of ubiquinone extraction and reconstitution, Biochem Biophys Res Commun 70 (1976) 839–845.
[25] M. Leonhard, W. Mantele, Fourier transform infrared spectroscopy and electrochemistry of the primary electron donor in *Rhodobacter sphaeroides* and *Rhodopseudomonas viridis* reaction centers — vibrational modes of the pigments *in situ* and evidence for protein and water modes affected by P^+ formation, Biochemistry 32 (1993) 4532–4538.
[26] A.B. Wohri, G. Katona, L.C. Johansson, E. Fritz, E. Malmerberg, M. Andersson, J. Vincent, M. Eklund, M. Cammarata, M. Wulff, J. Davidsson, G. Groenhof, R. Neutze, Light-induced structural changes in a photosynthetic reaction center caught by Laue diffraction, Science 328 (2010) 630–633.
[27] D. Kleinfeld, M.Y. Okamura, G. Feher, Electron transfer kinetics in photosynthetic reaction centers cooled to cryogenic temperatures in the charge-separated state — evidence for light induced structural changes, Biochemistry 23 (1984) 5780–5786.
[28] W. Nitschke, M. Dracheva, Reaction center associated cytochromes, in: R.E. Blankenship, M.T. Madigan, C.E. Bauer (Eds.), Anoxygenic photosynthetic bacteria: advances in photosynthesis, Kluwer Academic Publishers, Dordrecht, 1995, pp. 527–557.
[29] M.Y. Okamura, M.L. Paddock, M.S. Graige, G. Feher, Proton and electron transfer in bacterial reaction centers, Biochim Biophys Acta 1458 (2000) 148–163.
[30] C.A. Wraight, Proton and electron transfer in the acceptor quinone complex of photosynthetic reaction centers from *Rhodobacter sphaeroides*, Front Biosci 9 (2004) 309–337.
[31] B.A. Diner, F. Rappaport, Structure, dynamics, and energetics of the primary photochemistry of Photosystem II of oxygenic photosynthesis, Ann Rev Plant Biol 53 (2002) 551–580.
[32] J.P. Dekker, R. van Grondelle, Primary charge separation in Photosystem II, Photosynth Res 63 (2000) 195–208.
[33] F. Rappaport, B.A. Diner, Primary photochemistry and energetics leading to the oxidation of the $(Mn)_4Ca$ cluster and to the evolution of molecular oxygen in Photosystem II, Coord Chem Rev 252 (2008) 259–272.
[34] V.L. Teten'kin, B.A. Gulyaev, M. Seibert, A.B. Rubin, Spectral properties of stabilized D1/D2/cytochrome *b*559 Photosystem II reaction center complex — effects of Triton X-100, the redox state of pheophytin, and β-carotene, FEBS Lett 250 (1989) 459–463.
[35] P. Braun, B.M. Greenberg, A. Scherz, D1-D2-cytochrome *b*559 complex from the aquatic plant *Spirodela oligorrhiza* — correlation between complex integrity, spectroscopic properties, photochemical activity, and pigment composition, Biochemistry 29 (1990) 10376–10387.
[36] P.J.M. van Kan, S.C.M. Otte, F.A.M. Kleinherenbrink, M.C. Nieveen, T.J. Aartsma, H.J. van Gorkom, Time-resolved spectroscopy at 10 K of the Photosystem II reaction center — deconvolution of the red absorption band, Biochim Biophys Acta 1020 (1990) 146–152.
[37] J.R. Durrant, D.R. Klug, S.L.S. Kwa, R. van Grondelle, G. Porter, J.P. Dekker, A multimer model for P680, the primary electron donor of Photosystem II, Proc Natl Acad Sci U S A 92 (1995) 4798–4802.
[38] G. Raszewski, B.A. Diner, E. Schlodder, T. Renger, Spectroscopic properties of reaction center pigments in Photosystem II core complexes: revision of the multimer model, Biophys J 95 (2008) 105–119.
[39] Y. Umena, K. Kawakami, J.R. Shen, N. Kamiya, Crystal structure of the oxygen-evolving Photosystem II at a resolution of 1.9 Å, Nature 473 (2011) 55–60.
[40] A. Guskov, J. Kern, A. Gabdulkhakov, M. Broser, A. Zouni, W. Saenger, Cyanobacterial Photosystem II at 2.9 Å resolution and the role of quinones, lipids, channels and chloride, Nat Struct Mol Biol 16 (2009) 334–342.
[41] M.E.A. Madjet, F. Muh, T. Renger, Deciphering the influence of short-range electronic couplings on optical properties of molecular dimers: application to "special pairs" in photosynthesis, J Phys Chem B 113 (2009) 12603–12614.
[42] N. Cox, J.L. Hughes, R. Steffen, P.J. Smith, A.W. Rutherford, R.J. Pace, E. Krausz, Identification of the Q_Y excitation of the primary electron acceptor of Photosystem II: CD determination of its coupling environment, J Phys Chem B 113 (2009) 12364–12374.
[43] M.L. Groot, N.P. Pawlowicz, L. van Wilderen, J. Breton, I.H.M. van Stokkum, R. van Grondelle, Initial electron donor and acceptor in isolated Photosystem II reaction centers identified with femtosecond mid-IR spectroscopy, Proc Natl Acad Sci U S A 102 (2005) 13087–13092.
[44] A.R. Holzwarth, M.G. Muller, M. Reus, M. Nowaczyk, J. Sander, M. Rogner, Kinetics and mechanism of electron transfer in intact Photosystem II and in the isolated reaction center: pheophytin is the primary electron acceptor, Proc Natl Acad Sci U S A 103 (2006) 6895–6900.
[45] B.A. Diner, E. Schlodder, P.J. Nixon, W.J. Coleman, F. Rappaport, J. Lavergne, W.F.J. Vermaas, D.A. Chisholm, Site-directed mutations at D1-His198 and D2-His 97 of Photosystem II in *Synechocystis* PCC 6803: sites of primary charge separation and cation and triplet stabilization, Biochemistry 40 (2001) 9265–9281.
[46] I.V. Shelaev, F.E. Gostev, M.I. Vishnev, A.Y. Shkuropatov, V.V. Ptushenko, M.D. Mamedov, O.M. Sarkisov, V.A. Nadtochenko, A.Y. Semenov, V.A. Shuvalov, P_{680} ($P_{D1}P_{D2}$) and Chl_{D1} as alternative electron donors in Photosystem II core complexes and isolated reaction centers, J Photochem Photobiol B (2011), doi:10.1016/j.jphotobiol.2011.02.003.
[47] J.L. Hughes, P. Smith, R. Pace, E. Krausz, Charge separation in photosystem II core complexes induced by 690–730 nm excitation at 1.7 K, Biochim Biophys Acta 1757 (2006) 841–851.
[48] G. Raszewski, W. Saenger, T. Renger, Theory of optical spectra of Photosystem II reaction centers: location of the triplet state and the identity of the primary electron donor, Biophys J 88 (2005) 986–998.
[49] E. Schlodder, W.J. Coleman, P.J. Nixon, R.O. Cohen, T. Renger, B.A. Diner, Site-directed mutations at D1-His198 and D1-Thr179 of Photosystem II in *Synechocystis* sp PCC 6803: deciphering the spectral properties of the PSII reaction centre, Philos Trans R Soc B 363 (2008) 1197–1202.
[50] B.J. Hales, A. Dasgupta, Orientation of the bacteriochlorophyll triplet and the primary ubiquinone acceptor of *Rhodospirillum rubrum* in membrane multilayers determined by ESR spectroscopy (I), Biochim Biophys Acta 1979 (548) (1979) 276–286.
[51] D.M. Tiede, P.L. Dutton, Orientation of the primary quinone of bacterial photosynthetic reaction centers contained in chromatophore and reconstituted membranes/ion centers contained in chromatophore and reconstituted membranes, Biochim Biophys Acta 637 (1981) 278–290.
[52] A.W. Rutherford, P. Setif, Orientation of P700, the primary electron-donor of Photosystem I, Biochim Biophys Acta 1019 (1990) 128–132.
[53] W. Nitschke, U. Feiler, A.W. Rutherford, Photosynthetic reaction center of green sulfur bacteria studied by epr, Biochemistry 29 (1990) 3834–3842.
[54] W. Nitschke, P. Setif, U. Liebl, U. Feiler, A.W. Rutherford, Reaction center photochemistry of heliobacterium–chlorum, Biochemistry 29 (1990) 11079–11088.
[55] A. Zouni, H.T. Witt, J. Kern, P. Fromme, N. Krauss, W. Saenger, P. Orth, Crystal structure of Photosystem II from *Synechococcus elongatus* at 3.8 Å resolution, Nature 409 (2001) 739–743.

[56] N. Kamiya, J.R. Shen, Crystal structure of oxygen-evolving Photosystem II from *Thermosynechococcus vulcanus* at 3.7 Å resolution, Proc Natl Acad Sci U S A 100 (2003) 98–103.
[57] K.N. Ferreira, T.M. Iverson, K. Maghlaoui, J. Barber, S. Iwata, Architecture of the photosynthetic oxygen-evolving center, Science 303 (2004) 1831–1838.
[58] F.J.E. van Mieghem, K. Brettel, B. Hillmann, A. Kamlowski, A.W. Rutherford, E. Schlodder, Charge recombination reactions in Photosystem II.1. yields, recombination pathways, and kinetics of the primary pair, Biochemistry 34 (1995) 4798–4813.
[59] B. Hillmann, K. Brettel, F.J.E. van Mieghem, A. Kamlowski, A.W. Rutherford, E. Schlodder, Charge recombination reactions in Photosystem II .2. Transient absorbency difference spectra and their temperature-dependence, Biochemistry 34 (1995) 4814–4827.
[60] F.J.E. van Mieghem, W. Nitschke, P. Mathis, A.W. Rutherford, The influence of the quinone-iron electron-acceptor complex on the reaction center photochemistry of Photosystem II, Biochim Biophys Acta 977 (1989) 207–214.
[61] V. Martinez-Junza, M. Szczepaniak, S.E. Braslavsky, J. Sander, M. Nowaczyk, M. Rogner, A.R. Holzwarth, A photoprotection mechanism involving the D2 branch in Photosystem II cores with closed reaction centers, Photochem Photobiol Sci 7 (2008) 1337–1343.
[62] Y. Deligiannakis, J. Hanley, A.W. Rutherford, 1D- and 2D-ESEEM study of the semiquinone radical Q_A^- of Photosystem II, J Am Chem Soc 121 (1999) 7653–7664.
[63] E. Schlodder, B. Hillmann, K. Brettel, F. Mallwitz, $^3P_{680}$ in Photosystem II with singly reduced Q_A, in: G. Garab (Ed.), Photosynthesis: mechanisms and effects, Springer, Dordrecht, 1998, pp. 1069–1072.
[64] Y. Deligiannakis, A.W. Rutherford, Reaction centre photochemistry in cyanide-treated Photosystem II, Biochim Biophys Acta 1365 (1998) 354–362.
[65] T. Noguchi, Dual role of triplet localization on the accessory chlorophyll in the Photosystem II reaction center: photoprotection and photodamage of the D1 protein, Plant Cell Physiol 43 (2002) 1112–1116.
[66] W.O. Feikema, P. Gast, I.B. Klenina, I.I. Proskuryakov, EPR characterisation of the triplet state in Photosystem II reaction centers with singly reduced primary acceptor Q_A, Biochim Biophys Acta 2005 (1709) (2005) 105–112.
[67] E. Romero, I.H.M. van Stokkum, V.I. Novoderezhkin, J.P. Dekker, R. van Grondelle, Two different charge separation pathways in Photosystem II, Biochemistry 49 (2010) 4300–4307.
[68] P. Faller, C. Fufezan, A.W. Rutherford, Side-path donors: cytochrome *b*559, chlorophyll Z and β-carotene, in: T. Wydrzynski, K. Satoh (Eds.), Photosystem II: the light-driven water:plastoquinone oxidoreductase, Springer, Dordrecht, 2005, pp. 347–365.
[69] C.A. Tracewell, J.S. Vrettos, J.A. Bautista, H.A. Frank, G.W. Brudvig, Carotenoid photooxidation in Photosystem II, Arch Biochem Biophys 385 (2001) 61–69.
[70] G. Renger, A.R. Holzwarth, Primary electron transfer, in: T. Wydrzynski, K. Satoh (Eds.), Photosystem II: the light-driven water:plastoquinone oxidoreductase, Springer, Dordrecht, 2005, pp. 139–175.
[71] H.J. van Gorkom, Electron transfer in Photosystem II, Photosynth Res 6 (1985) 97–112.
[72] G.N. Johnson, A.W. Rutherford, A. Krieger, A change in the midpoint potential of the quinone Q_A in Photosystem II associated with photoactivation of oxygen evolution, Biochim Biophys Acta 1229 (1995) 202–207.
[73] F. Rappaport, M. Guergova-Kuras, P.J. Nixon, B.A. Diner, J. Lavergne, Kinetics and pathways of charge recombination in Photosystem II, Biochemistry 41 (2002) 8518–8527.
[74] Y. Kato, M. Sugiura, A. Oda, T. Watanabe, Spectroelectrochemical determination of the redox potential of pheophytin a, the primary electron acceptor in Photosystem II, Proc Natl Acad Sci U S A 106 (2009) 17365–17370.
[75] S.I. Allakhverdiev, T. Tomo, Y. Shimada, H. Kindo, R. Nagao, V.V. Klimov, M. Mimuro, Redox potential of pheophytin a in Photosystem II of two cyanobacteria having the different special pair chlorophylls, Proc Natl Acad Sci U S A 107 (2010) 3924–3929.
[76] S. Un, X.S. Tang, B.A. Diner, 245 GHz high-field EPR study of tyrosine-D$^\bullet$ and tyrosine-Z$^\bullet$ in mutants of Photosystem II, Biochemistry 35 (1996) 679–684.
[77] B.A. Diner, R.D. Britt, The redox active Tyrosines Y_Z and Y_D, in: T. Wydrzynski, K. Satoh (Eds.), Photosystem II: the light-driven water:plastoquinone oxidoreductase, Springer, Dordrecht, 2005, pp. 207–233.
[78] F. Rappaport, M. Blancharddesce, J. Lavergne, Kinetics of electron-transfer and electrochromic change during the redox transitions of the photosynthetic oxygen-evolving complex, Biochim Biophys Acta 1184 (1994) 178–192.
[79] M.R. Razeghifard, C. Klughammer, R.J. Pace, Electron paramagnetic resonance kinetic studies of the S states in spinach thylakoids, Biochemistry 36 (1997) 86–92.
[80] R. de Wijn, H.J. van Gorkom, Kinetics of electron transfer from Q_A to Q_B in Photosystem II, Biochemistry 40 (2001) 11912–11922.
[81] V. Petrouleas, A.R. Crofts, The iron-quinone acceptor complex, in: T. Wydrzynski, K. Satoh (Eds.), Photosystem II: the light-driven water:plastoquinone oxidoreductase, Springer, Dordrecht, 2005, pp. 177–206.
[82] F.A. Wollman, Determination and modification of redox state of secondary acceptor of Photosystem II in dark, Biochim Biophys Acta 503 (1978) 263–273.
[83] A.W. Rutherford, A.R. Crofts, Y. Inoue, Thermoluminescence as a probe of Photosystem II photochemistry — the origin of the flash-induced glow peaks, Biochim Biophys Acta 682 (1982) 457–465.
[84] H.H. Robinson, A.R. Crofts, Kinetics of the oxidation reduction reactions of the Photosystem II quinone acceptor complex, and the pathway for deactivation, FEBS Lett 153 (1983) 221–226.
[85] H. Ishikita, W. Saenger, J. Biesiadka, B. Loll, E.W. Knapp, How photosynthetic reaction centers control oxidation power in chlorophyll pairs P680, P700, and P870, Proc Natl Acad Sci U S A 103 (2006) 9855–9860.
[86] J. Fajer, D.C. Brune, M. Davis, A. Forman, L.D. Spaulding, Primary charge separation in bacterial photosynthesis — oxidized chlorophylls and reduced pheophytin, Proc Natl Acad Sci U S A 72 (1975) 4956–4960.
[87] R. Takahashi, K. Hasegawa, T. Noguchi, Effect of charge distribution over a chlorophyll dimer on the redox potential of P680 in Photosystein II as studied by density functional theory calculations, Biochemistry 47 (2008) 6289–6291.
[88] A.W. Rutherford, P. Faller, Photosystem II: evolutionary perspectives, Philos Philos Trans R Soc B 358 (2003) 245–253.
[89] G.C. Dismukes, R.E. Blankenship, The origin and evolution of photosynthetic oxygen production, in: T. Wydrzynski, K. Satoh (Eds.), Photosystem II: the light-driven water:plastoquinone oxidoreductase, Springer, Dordrecht, 2005, pp. 683–695.
[90] H.J. van Gorkom, Evolution of photosynthesis, in: J. Amesz (Ed.), New Comprenhensive Biochemistry, Vol. 15, Elsevier, Amsterdam, 1987, pp. 343–350.
[91] H.H. Stiehl, H.T. Witt, Quantitative treatment of function of plastoquinone in photosynthesis, Z Naturforsch Pt B 24 (1969) 1588–1598.
[92] H.J. van Gorkom, Identification of reduced primary electron-acceptor of Photosystem II as a bound semiquinone anion, Biochim Biophys Acta 347 (1974) 439–442.
[93] R.K. Clayton, S.C. Straley, Photochemical electron-transport in photosynthetic reaction centers.4. Observations related to reduced photoproducts, Biophys J 12 (1972) 1221–1234.
[94] G. Feher, R.A. Isaacson, J.D. McElroy, L.C. Ackerson, M.Y. Okamura, Question of primary acceptor in bacterial photosynthesis — manganese substituting for iron in reaction centers of *Rhodopseudomonas spheroides* R-26, Biochim Biophys Acta 368 (1974) 135–139.
[95] B. Bouges-Bocquet, Electron-transfer between 2 photosystems in spinach chloroplasts, Biochim Biophys Acta 314 (1973) 250–256.
[96] B.R. Velthuys, J. Amesz, Charge accumulation at reducing side of System 2 of photosynthesis, Biochim Biophys Acta 333 (1974) 85–94.
[97] C.A. Wraight, Electron-acceptors of photosynthetic bacterial reaction centers — direct observation of oscillatory behavior suggesting 2 closely equivalent ubiquinones, Biochim Biophys Acta 459 (1977) 525–531.
[98] A. Vermeglio, R.K. Clayton, Kinetics of electron transfer between primary and secondary electron acceptor in reaction centers from *Rhodopseudomonas sphaeroides*, Biochim Biophys Acta 461 (1977) 159–165.
[99] V.V. Klimov, A.V. Klevanik, V.A. Shuvalov, A.A. Krasnovsky, Reduction of pheophytin in primary light reaction of Photosystem 2, FEBS Lett 82 (1977) 183–186.
[100] V.V. Klimov, E. Dolan, E.R. Shaw, B. Ke, Interaction between the intermediary electron-acceptor (pheophytin) and a possible plastoquinone–iron complex in Photosystem II reaction centers, Proc Natl Acad Sci Biol 77 (1980) 7227–7231.
[101] D.M. Tiede, R.C. Prince, G.H. Reed, P.L. Dutton, EPR properties of electron carrier intermediate between reaction center bacteriochlorophylls and primary acceptor in *Chromatium vinosum*, FEBS Lett 65 (1976) 301–304.
[102] A.W. Rutherford, D.R. Paterson, J.E. Mullet, A light-induced spin-polarized triplet detected by electron paramagnetic res in Photosystem II reaction centers, Biochim Biophys Acta 635 (1981) 205–214.
[103] P.L. Dutton, J.S. Leigh, D.W. Reed, Primary events in photosynthetic reaction center from *Rhodopseudomonas spheroides* strain R26 — Triplet and oxidized states of bacteriochlorophyll and identification of primary electron-acceptor, Biochim Biophys Acta 292 (1973) 654–664.
[104] J.S. Leigh, P.L. Dutton, Reaction center bacteriochlorophyll triplet states — redox potential dependence and kinetics, Biochim Biophys Acta 1974 (357) (1974) 67–77.
[105] M.C. Thurnauer, J.J. Katz, J.R. Norris, Triplet-state in bacterial photosynthesis — possible mechanisms of primary photo-act, Proc Natl Acad Sci U S A 72 (1975) 3270–3274.
[106] A.W. Rutherford, J.E. Mullet, D.R. Paterson, H.H. Robinson, C.J. Arntzen, A.R. Crofts, Some biophysical properties of purified PSI and PSII particles, in: G. Akoyunoglou (Ed.), Proceedings of the Fifth International Photosynthesis Congress, Balaban International Science Services, Philadelphia, Photosynthesis, 1981, pp. 919–928.
[107] V.A. Shuvalov, V.V. Klimov, E. Dolan, W.W. Parson, B. Ke, Nanosecond fluorescence and absorbance changes in Photosystem II at low redox potential — pheophytin as an intermediary electron acceptor, FEBS Lett 118 (1980) 279–282.
[108] J.H.A. Nugent, B.A. Diner, M.C.W. Evans, Direct detection of the electron-acceptor of Photosystem II — evidence that Q is an iron–quinone complex, FEBS Lett 124 (1981) 241–244.
[109] A.W. Rutherford, P. Mathis, A relationship between the midpoint potential of the primary acceptor and low-temperature photochemistry in Photosystem II, FEBS Lett 154 (1983) 328–334.
[110] W.F.J. Vermaas, A.W. Rutherford, Electron paramagnetic res measurements on the effects of bicarbonate and triazine resistance on the acceptor side of Photosystem II, FEBS Lett 175 (1984) 243–248.
[111] A.W. Rutherford, J.L. Zimmermann, A new electron paramagnetic res signal attributed to the primary plastosemiquinone acceptor in Photosystem II, Biochim Biophys Acta 767 (1984) 168–175.
[112] A.W. Rutherford, How close is the analogy between the reaction centre of Photosystem II and that of purple bacteria? The electron acceptors side, in: J. Biggins (Ed.), Progress in photosynthesis research, Nijhoff, The Hague, 1987, pp. 277–283.
[113] R. Hienerwadel, C. Berthomieu, Bicarbonate binding to the non-heme iron of Photosystem II investigated by Fourier transform infrared difference spectroscopy and C^{13}-labeled bicarbonate, Biochemistry 34 (1995) 16288–16297.

[114] N. Cox, L. Jin, A. Jaszewski, P.J. Smith, E. Krausz, A.W. Rutherford, R. Pace, The semiquinone–iron complex of Photosystem II: structural insights from ESR and theoretical simulation; evidence that the native ligand to the non-heme iron is carbonate, Biophys J 97 (2009) 2024–2033.
[115] J. Deisenhofer, O. Epp, K. Miki, R. Huber, H. Michel, Structure of the protein subunits in the photosynthetic reaction center of *Rhodopseudomonas viridis* at 3 Å resolution, Nature 318 (1985) 618–624.
[116] A. Trebst, W. Draber, Inhibitors of Photosystem II and the topology of the herbicide and Q_B binding polypeptide in the thylakoid membrane, Photosynth Res 10 (1986) 381–392.
[117] J. Barber, J.B. Marder, Photosynthesis and the application of molecular genetics, in: biotechnology and genetic engineering reviews 4, Interceot Ltd., Newcaste-upon-Tyne, 1986, pp. 355–404.
[118] R.T. Sayre, B. Andersson, L. Bogorad, The topology of a membrane protein — the orientation of the 32 kD Q_B binding chloroplast thylakoid membrane protein, Cell 47 (1986) 601–608.
[119] O. Nanba, K. Satoh, Isolation of a Photosystem II reaction center consisting of D1 and D2 polypeptides and cytochrome *b*559, Proc Natl Acad Sci U S A 84 (1987) 109–112.
[120] R.J. Debus, B.A. Barry, G.T. Babcock, L. McIntosh, Site-directed mutagenesis identifies a tyrosine radical involved in the photosynthetic oxygen-evolving system, Proc Natl Acad Sci U S A 85 (1988) 427–430.
[121] W.F.J. Vermaas, A.W. Rutherford, O. Hansson, Site-directed mutagenesis in Photosystem II of the cyanobacterium *Synechocystis* sp PCC 6803 — donor-D is a tyrosine residue in the D2-protein, Proc Natl Acad Sci U S A 85 (1988) 8477–8481.
[122] B. Svensson, I. Vass, E. Cedergren, S. Styring, Structure of donor side components in Photosystem II predicted by computer modeling, EMBO J 9 (1990) 2051–2059.
[123] P. Dorlet, A.W. Rutherford, S. Un, Orientation of the tyrosyl D, pheophytin anion, and semiquinone $Q_A^{\bullet}$ radicals in Photosystem II determined by high-field electron paramagnetic resonance, Biochemistry 39 (2000) 7826–7834.
[124] R. Bittl, A. Kawamori, Configuration of electron transport components studied by EPR spectroscopy, in: T. Wydrzynski, S. Satoh (Eds.), Photosystem II: the light-driven water:plastoquinone oxidoreductase, Springer, Dordrecht, 2005, pp. 389–402.
[125] Y. Deligiannakis, A.W. Rutherford, Spin-lattice relaxation of the pheophytin, $Pheo^{-}$, radical of Photosystem II, Biochemistry 35 (1996) 11239–11246.
[126] D. Koulougliotis, X.S. Tang, B.A. Diner, G.W. Brudvig, Spectroscopic evidence for the symmetrical location of tyrosine-D and tyrosine-Z in Photosystem II, Biochemistry 34 (1999) 2850–2856.
[127] S.G. Zech, J. Kurreck, H.J. Eckert, G. Renger, W. Lubitz, R. Bittl, Pulsed EPR measurement of the distance between P-$680^{+\bullet}$ and $Q_A^{-\bullet}$ in Photosystem II, FEBS Lett 414 (1997) 454–456.
[128] K.H. Rhee, E.P. Morris, D. Zheleva, B. Hankamer, W. Kuhlbrandt, J. Barber, Two-dimensional structure of plant Photosystem II at 8 Å resolution, Nature 389 (1997) 522–526.
[129] B. Loll, J. Kern, W. Saenger, A. Zouni, J. Biesiadka, Towards complete cofactor arrangement in the 3.0 Å resolution structure of Photosystem II, Nature 438 (2005) 1040–1044.
[130] T.J. Beanland, Evolutionary relationships between q-type photosynthetic reaction centers — hypothesis-testing using parsimony, J Theor Biol 145 (1990) 535–545.
[131] M.H.B. Stowell, T.M. McPhillips, D.C. Rees, S.M. Soltis, E. Abresch, G. Feher, Light-induced structural changes in photosynthetic reaction center: implications for mechanism of electron-proton transfer, Science 276 (1997) 812–816.
[132] E. Nabedryk, J. Breton, Coupling of electron transfer to proton uptake at the Q_B site of the bacterial reaction center: a perspective from FTIR difference spectroscopy, Biochim Biophys Acta 1777 (2008) 1229–1248.
[133] E. Martin, R.I. Samoilova, K.V. Narasimhulu, T.J. Lin, P.J. O'Malley, C.A. Wraight, S.A. Dikanov, Hydrogen bonding and spin density distribution in the Q_B semiquinone of bacterial reaction centers and comparison with the Q_A site, J. Am. Chem. Soc. 133 (2011) 5525–5537.
[134] M.L. Paddock, M. Flores, R. Isaacson, C. Chang, E.C. Abresch, M.Y. Okamura, ENDOR spectroscopy reveals light induced movement of the H-bond from Ser-L223 upon forming the semiquinone $Q_B^{-\bullet}$ in reaction centers from *Rhodobacter sphaeroides*, Biochemistry 46 (2007) 8234–8243.
[135] D. Onidas, J.M. Stachnik, S. Brucker, S. Kratzig, K. Gerwert, Histidine is involved in coupling proton uptake to electron transfer in photosynthetic proteins, Eur J Cell Biol 89 (2010) 983–989.
[136] P. Chernev, I. Zaharieva, H. Dau, M. Haumann, Carboxylate shifts steer interquinone electron transfer in photosynthesis, J Biol Chem 286 (2011) 5368–5374.
[137] H. Suzuki, M. Nagasaka, M. Sugiura, T. Noguchi, Fourier transform infrared spectrum of the secondary quinone electron acceptor Q_B in Photosystem II, Biochemistry 44 (2005) 11323–11328.
[138] F. Reifarth, G. Renger, Indirect evidence for structural changes coupled with $Q_B^{-\bullet}$ formation in Photosystem II, FEBS Lett 428 (1998) 123–126.
[139] A. Garbers, F. Reifarth, J. Kurreck, G. Renger, F. Parak, Correlation between protein flexibility and electron transfer from $Q_A^{-\bullet}$ to Q_B in PSII membrane fragments from spinach, Biochemistry 37 (1998) 11399–11404.
[140] C. Fufezan, C.X. Zhang, A. Krieger-Liszkay, A.W. Rutherford, Secondary quinone in Photosystem II of *Thermosynechococcus elongatus*: semiquinone-iron EPR signals and temperature dependence of electron transfer, Biochemistry 44 (2005) 12780–12789.
[141] C.C. Moser, C.C. Page, P.L. Dutton, Tunneling in PSII, Photochem Photobiol Sci 4 (2005) 933–939.
[142] R.J. Debus, G. Feher, M.Y. Okamura, Iron-depleted reaction centers from *Rhodopseudomonas sphaeroides* R-26.1 — characterization and reconstitution with Fe^{2+}, Mn^{2+}, Co^{-2+}, Ni^{-2+}, Cu^{-2+}, and Zn^{-2+}, Biochemistry 25 (1986) 2276–2287.
[143] H. Ishikita, E.-W. Knapp, Electrostatic role of the non-heme iron complex in bacterial photosynthetic reaction center, FEBS Lett 580 (2006) 4567–4570.
[144] T.J. Lin, An ONIOM study of the spin density distribution of the Q_A site plastosemiquinone in the Photosystem II reaction centre, in: P.J. O'Malley (Ed.), J Phys Chem B 115 (2011) 4227–4233.
[145] A. Krieger, E. Weis, S. Demeter, Low-ph-induced Ca^{2+} ion release in the water-splitting system is accompanied by a shift in the midpoint redox potential of the primary quinone acceptor Q_A, Biochim Biophys Acta 1144 (1993) 411–418.
[146] A. Krieger, A.W. Rutherford, G.N. Johnson, On the determination of redox midpoint potential of the primary quinone electron-acceptor, Q_A, in Photosystem II, Biochim Biophys Acta 1229 (1995) 193–201.
[147] T. Shibamoto, Y. Kato, M. Sugiura, T. Watanabe, Redox potential of the primary plastoquinone electron acceptor Q_A in Photosystem II from *Thermosynechococcus elongatus* determined by spectroelectrochemistry, Biochemistry 48 (2009) 10682–10684.
[148] K. Ido, C.M. Gross, F. Guerrero, A. Sedoud, T.-L. Lai, K. Ifuku, A.W. Rutherford, A. Krieger-Liszkay, High and low potential forms of the Q_A quinone electron acceptor in Photosystem II of *Thermosynechococcus elongatus* and spinach, J Photochem Photobiol B (2011), doi:10.1016/j.jphotobiol.2011.02.010.
[149] C.A. Tracewell, G.W. Brudvig, Multiple redox-active chlorophylls in the secondary electron transfer pathways of oxygen evolving Photosystem II, Biochemistry 47 (2008) 11559–11572.
[150] N. Keren, A. Berg, P.J.M. van Kan, H. Levanon, I. Ohad, Mechanism of Photosystem II photoinactivation and D1 protein degradation at low light: the role of back electron flow, Proc Natl Acad Sci U S A 94 (1997) 1579–1584.
[151] C. Fufezan, A.W. Rutherford, A. Krieger-Liszkay, Singlet oxygen production in herbicide-treated Photosystem II, FEBS Lett 532 (2002) 407–410.
[152] N. Mizusawa, T. Yamashita, M. Miyao, Restoration of the high-potential form of cytochrome *b*559 of Photosystem II occurs via a two-step mechanism under illumination in the presence of manganese ions, Biochim Biophys Acta 1410 (1999) 273–286.
[153] V.P. McNamara, K. Gounaris, Granal Photosystem II complexes contain only the high redox potential form of cytochrome b-559 which is stabilized by the ligation of calcium, Biochim Biophys Acta 1231 (1995) 289–296.
[154] A. Gopher, Y. Blatty, D.M. Schonfeld, M.Y. Okamura, G. Feher, M. Montal, The effect of an applied elelctric field on the charge recombination kinetics in reaction centers reconstitutes in planar lipid bilayers, Biophys J 48 (1985) 311–320.
[155] R.J. Shopes, C.A. Wraight, Charge recombination from the $P^{+}Q_A^{-}$ state in reaction centers from *Rhodopseudomonas viridis*, Biochim Biophys Acta 893 (1987) 409–425.
[156] N.W. Woodbury, W.W. Parson, M.R. Gunner, R.C. Prince, P.L. Dutton, Radical-pair energetics and decay mechanisms in reaction centers containing anthraquinones, naphthoquinones or benzoquinones in place of ubiquinone, Biochim Biophys Acta 851 (1986) 6–22.
[157] H. Ishikita, E.W. Knapp, Control of quinone redox potentials in Photosystem II: electron transfer and photoprotection, J Am Chem Soc 127 (2005) 14714–14720.
[158] A. Krieger-Liszkay, A.W. Rutherford, Influence of herbicide binding on the redox potential of the quinone acceptor in Photosystem II. Relevance to photodamage and phytotoxicity, Biochemistry 37 (1998) 17339–17344.
[159] C.G. Chen, J. Kazimir, G.M. Cheniae, Calcium modulates the photoassembly of photosystem II Mn_4-clusters by preventing ligation of non-functional high-valency states of manganese, Biochemistry 34 (1995) 13511–13526.
[160] N. Tamura, G.M. Cheniae, Photoactivation of the water-oxidizing complex in Photosystem II membranes depleted of mn and extrinsic proteins.1. Biochemical and kinetic characterization, Biochim Biophys Acta 890 (1987) 179–194.
[161] N. Tamura, Y. Inoue, G.M. Cheniae, Photoactivation of the water-oxidizing complex in Photosystem II membranes depleted of Mn, Ca and extrinsic proteins.2. Studies on the functions of Ca2+, Biochim Biophys Acta 976 (1989) 173–181.
[162] A. Boussac, J.L. Zimmermann, A.W. Rutherford, Factors influencing the formation of modified S_2 EPR signal and the S_3 EPR signal in Ca^{2+}-depleted Photosystem II, FEBS Lett 277 (1990) 69–74.
[163] Y.L. Pushkar, J. Yano, K. Sauer, A. Boussac, V.K. Yachandra, Structural changes in the Mn_4Ca cluster and the mechanism of photosynthetic water splitting, Proc Natl Acad Sci U S A 105 (2008) 1879–1884.
[164] A. Gauthier, D. Joly, S. Boisvert, R. Carpentier, Period-four modulation of Photosystem II primary quinone acceptor (Q_A) reduction/oxidation kinetics in thylakoid membranes, Photochem Photobiol 86 (2010) 1064–1070.
[165] J. Kern, B. Loll, C. Luneberg, D. DiFiore, J. Biesiadka, K.D. Irrgang, A. Zouni, Purification, characterisation and crystallisation of Photosystem II from *Thermosynechococcus elongatus* cultivated in a new type of photobioreactor, Biochim Biophys Acta 1706 (2005) 147–157.
[166] O. Kaminskaya, V.A. Shuvalov, G. Renger, Evidence for a novel quinone-binding site in the photosystem II (PS II) complex that regulates the redox potential of cytochrome *b*559, Biochemistry 46 (2007) 1091–1105.
[167] J. Kruk, K. Strzalka, Dark reoxidation of the plastoquinone-pool is mediated by the low-potential form of cytochrome *b*559 in spinach thylakoids, Photosynth Res 62 (1999) 273–279.
[168] A. Tiwari, P. Pospisil, Superoxide oxidase and reductase activity of cytochrome *b*559 in Photosystem II, Biochim Biophys Acta 1787 (2009) 985–994.
[169] N. Bondarava, C.M. Gross, M. Mubarakshina, J.R. Golecki, G.N. Johnson, A. Krieger-Liszkay, Putative function of cytochrome *b*559 as a plastoquinol oxidase, Physiol Plant 138 (2010) 463–473.

[170] J. Hanley, Y. Deligiannakis, A. Pascal, P. Faller, A.W. Rutherford, Carotenoid oxidation in Photosystem II, Biochemistry 38 (1999) 8189–8195.
[171] C.A. Buser, B.A. Diner, G.W. Brudvig, Photooxidation of cytochrome b559 in oxygen-evolving Photosystem II, Biochemistry 31 (1992) 11449–11459.
[172] L.K. Thompson, G.W. Brudvig, Cytochrome *b*559 may function to protect Photosystem II from photoinhibition, Biochemistry 27 (1988) 6653–6658.
[173] O. Prasil, Z. Kolber, J.A. Berry, P.G. Falkowski, Cyclic electron flow around Photosystem II *in vivo*, Photosynth Res 48 (1996) 395–410.
[174] W.O. Feikema, M.A. Marosvolgyi, J. Lavaud, H.J. van Gorkom, Cyclic electron transfer in Photosystem II in the marine diatom *Phaeodactylum tricornutum*, Biochim Biophys Acta 1757 (2006) 829–834.
[175] D.H. Stewart, G.W. Brudvig, Cytochrome *b*559 of Photosystem II, Biochim Biophys Acta 1367 (1998) 63–87.
[176] A. Telfer, J.D. Rivas, J. Barber, β-carotene within the isolated Photosystem II reaction center — photooxidation and irreversible bleaching of this chromophore by oxidized P680, Biochim Biophys Acta 1060 (1991) 106–114.
[177] H. Ishikita, B. Loll, J. Biesiadka, J. Kern, K.D. Irrgang, K.A. Zouni, W. Saenger, E.W. Knapp, Function of two β-carotenes near the D1 and D2 proteins in Photosystem II dimers, Biochim Biophys Acta 1767 (2007) 79–87.
[178] F. Guerrero, A. Sedoud, D. Kirilovsky, A.W. Rutherford, J.M. Ortega, M. Roncel, A high redox potential form of Cytochrome c550 in Photosystem II from *Thermosynechococcus elongatus*, J Biol Chem 286 (2011) 5985–5994.
[179] J.W. Murray, K. Maghlaoui, J. Barber, The structure of allophycocyanin from *Thermosynechococcus elongatus* at 3.5 Å resolution, Acta Crystallogr F 63 (2007).
[180] V. Petrouleas, B.A. Diner, Identification of Q_{400}, a high potential electron acceptor of Photosystem II, with the iron of the quinone–iron acceptor complex, Biochim Biophys Acta 849 (1986) 264–275.
[181] V. Petrouleas, Y. Deligiannakis, B.A. Diner, Binding of carboxylate anions at the nonheme FeII of PS-II.2. Competition with bicarbonate and effects on the QA/QB electron-transfer rate, Biochim Biophys Acta 1188 (1994) 271–277.
[182] J.L. Zimmermann, A.W. Rutherford, Photoreductant induced oxidation of Fe^{2+} in the electron acceptor complex of Photosystem II, Biochim Biophys Acta 851 (1986) 416–423.
[183] J.H.A. Nugent, Photoreducible high spin iron electron paramagnetic resonance signals in dark-adapted Photosystem II: are they oxidised non-haem iron formed from interaction of oxygen with PSII electron acceptors? Biochim Biophys Acta 1504 (2001) 288–298.
[184] A. Boussac, M. Sugiura, F. Rappaport, Probing the quinone binding site of Photosystem II from *Thermosynechococcus elongatus* containing either PsbA1 or PsbA3 as the D1 protein through the binding characteristics of herbicides, Biochim Biophys Acta 1807 (2011) 119–129.
[185] A. Sedoud, Transfert d'électrons dans le photosystème II, These de doctorat de l'Universite Paris Sud – 11, Paris, 2011.
[186] C. Beijer, A.W. Rutherford, The iron–quinone acceptor complex in *Rhodospirillum rubrum* chromatophores studied by electron paramagnetic resonance, Biochim Biophys Acta 890 (1987) 169–178.
[187] R.J. Shopes, D.J. Blubaugh, C.A. Wraight, Govindjee, Absence of a bicarbonate-depletion effect in electron-transfer between quinones in chromatophores and reaction centers of *Rhodobacter sphaeroides*, Biochim Biophys Acta 974 (1989) 114–118.
[188] P. Jursinic, J. Warden, Govindjee, Major site of bicarbonate effect in system-II reaction evidence from ESR signal-IIvf, fast fluorescence yield changes and delayed light-emission, Biochim Biophys Acta 440 (1976) 322–330.
[189] U. Siggel, R. Khanna, G. Renger, Govindjee, Investigation of absorption changes of plastoquinone system in broken chloroplasts — Effect of bicarbonate depletion, Biochim Biophys Acta 462 (1977) 196–207.
[190] H.H. Robinson, J.J. Eaton-Rye, J.J.S. van Rensen, Govindjee, The effects of bicarbonate depletion and formate incubation on the kinetics of oxidation-reduction reactions of the Photosystem II quinone acceptor complex, Z Naturforsch C 39 (1984) 382–385.
[191] J.J.S. van Rensen, V.V. Klimov, Bicarbonate interactions, in: T. Wydrzynski, S. Satoh (Eds.), Photosystem II: the light-driven water:plastoquinone oxidoreductase, Springer, Dordrecht, 2005, pp. 329–346.
[192] A. Sedoud, L. Kastner, N. Cox, S. El-Alaoui, D. Kirilovsky, A.W. Rutherford, Effects of formate binding on the quinone–iron electron acceptor complex of Photosystem II, Biochim Biophys Acta 1807 (2011) 216–226.
[193] R. De Wijn, H.J. van Gorkom, The rate of charge recombination in Photosystem II, Biochim. Biophys. Acta 1553 (2002) 302–308.